H3K27me3 is dispensable for early differentiation but required to maintain differentiated cell identity

Sara A. Miller[1,2], Manashree Damle[1], Robert E. Kingston[1,2,*]

AFFILIATIONS:

[1]Department of Molecular Biology, Massachusetts General Hospital Research Institute, Massachusetts General Hospital, Boston, Massachusetts 02114, USA

[2]Department of Genetics, Harvard Medical School, Boston, Massachusetts 02115, USA

*Correspondence: kingston@molbio.mgh.harvard.edu

Abstract

Polycomb repressive complex 2 (PRC2) catalyzes trimethylation of histone H3 on lysine 27 and is required for normal development of complex eukaryotes. The requirement for H3K27me3 in various aspects of mammalian differentiation is not clear. Though associated with repressed genes, the modification is not sufficient to induce gene repression, and in some instances is not required. To examine the role of the modification in mammalian differentiation, we blocked trimethylation of H3K27 with both a small molecule inhibitor, GSK343, and by introducing a point mutation into EZH2, the catalytic subunit of PRC2. We found that cells with substantively decreased H3K27 tri-methylation were able to differentiate, which contrasts with EZH2 null cells. Different PRC2 targets had varied requirements for H3K27me3 in repressive regulation with a subset that maintained normal levels of repression in the absence of methylation. The primary cellular phenotype when H3K27 tri-methylation was blocked was an inability of the altered cells to maintain a differentiated state when challenged. This phenotype was determined by H3K27me3 deposition both in embryonic stem cells and in the first four days of differentiation. H3K27 tri-methylation therefore was not necessary for formation of differentiated cell states but was required to maintain a stable differentiated state.

31 **Introduction**

32

33 Polycomb repressive complex 2 (PRC2) is a highly conserved protein complex that is
34 required for proper axial patterning of vertebrates. It is comprised of the core subunits EZH2,
35 SUZ12, EED and RBAP48, with additional subunits some of which are cell-type or developmental
36 stage specific (Healy et al., 2019; Margueron & Reinberg, 2011; Shen et al., 2009; van Mierlo et
37 al., 2019). The complex is crucial for differentiation, but it is not required for the self-renewing
38 phenotype associated with embryonic stem (ES) cells (Aloia et al., 2013; Chamberlain et al.,
39 2008). At a molecular level, PRC2 family complexes are the only histone 3 lysine 27 (H3K27)
40 methyltransferases identified in mammals. EZH2 is the primary catalytic component of these
41 complexes, with its paralog EZH1 also contributing to catalytic activity in some instances
42 (Margueron et al., 2008; Shen et al., 2008; Wassef et al., 2019; Xu et al., 2015). Lysine residues
43 can be mono- di- or tri- methylated, with PRC2 able to catalyze all levels of methylation.
44 Increased methylation is generally associated with gene repression, and H3K27 tri-methylation
45 (H3K27me3) is a key marker of facultative heterochromatin. However, the tri-methylation of
46 H3K27 is neither required nor sufficient to induce gene repression (Ahmed et al., 2018;
47 Chamberlain et al., 2008; Ferguson et al., 2018; O'Geen et al., 2017). Dissecting the role of tri-
48 methylated H3K27 in gene regulation is important for understanding how genes become
49 repressed during development and retain their repression in differentiated cells.

50

51 Changes in expression level or activity of Polycomb complexes have developmental and
52 disease effects. Both hyper-activating and inactivating mutations in PRC2 have been identified
53 from a variety of human cancers (Basheer et al., 2019; Cyrus et al., 2019; Jain & Di Croce, 2016).
54 Malignancies with both types of alterations to PRC2 function have been linked to cancer
55 progression and poor prognosis in a wide variety of tissue (Abdel Raouf et al., 2019; Basheer et
56 al., 2019; Bohm et al., 2019; Bremer et al., 2019; Deng et al., 2019; Dou et al., 2019; Karlowee
57 et al., 2019; Krill et al., 2020; Matsubara et al., 2019; Mechaal et al., 2019; Shi et al., 2019; Tian
58 et al., 2019; Wasenang et al., 2019; M. J. Zhang et al., 2019; Q. Zhang et al., 2019). These
59 findings are consistent with the initial identification of Polycomb-Group genes in Drosophila

60 where haploinsufficiency yielded developmental phenotypes (Lewis & Mislove, 1947;
61 Schuettengruber et al., 2017). Inserting these disease mutations into cells alters the
62 modification profiles of H3K27 and can change their developmental potential. Increased
63 methylation can often push cells toward a neuro progenitor phenotype (Juan et al., 2016; Pasini
64 et al., 2007; Thornton et al., 2014). In cancer patients, increased levels of expression of PRC2
65 components and especially EZH2 leads to hypermethylation and is associated with poor
66 prognosis (Tian et al., 2019; Wu et al., 2019). Consequently, there is significant interest in
67 targeting this complex pharmaceutically. Small molecules that inhibit PRC2 methyltransferase
68 activity have been approved for clinical trials (Fioravanti et al., 2018; Kondo, 2014; Liu et al.,
69 2015; Lue & Amengual, 2018; Qi et al., 2012; Shi et al., 2019; Xu et al., 2015; Yamagishi &
70 Uchimaru, 2017; Yang et al., 2019). It remains, however, unclear how far this activity can be
71 manipulated before risking adverse effects from having too little of the modification present.
72 The ambiguity of the role of H3K27me3 in disease progression increases the importance of
73 understanding the mechanisms by which PRC2 methylation activities regulate gene expression
74 during development.
75
76 Previous work on PRC2 has shown that the complex is dispensable for the propagation
77 of self-renewing, undifferentiated cells that are phenotypically indistinguishable from WT ES
78 cells. These studies have also shown that PRC2 deficient cells do not differentiate properly
79 (Chamberlain et al., 2008; Lavarone et al., 2019; Pasini et al., 2007; Pasini et al., 2004; Shen et
80 al., 2008). Since the entire complex is disrupted when any of the core components are knocked
81 out, it is not clear whether it is solely the lack of methylation that is causing these
82 developmental defects, or whether there are other mechanistic roles PRC2 plays that are
83 distinct from methylation(Collinson et al., 2016; Rai et al., 2013; Shan et al., 2017; Yu et al.,
84 2017). A recent study examined the impact of a mutation in *Ezh2* that blocks all levels of
85 methylation. When these cells were differentiated into embryoid bodies they showed visual
86 phenotypic differences (Lavarone et al., 2019), demonstrating that complete removal of the
87 methyltransferase activity of PRC2 impairs normal differentiation. We focus here on the

88 developmental phenotypes caused by specific loss of the H3K27me3 modification, as opposed
89 to loss of all methylation.
90
91 To determine the contribution that H3K27me3 makes to gene repression, we examined
92 cells with a point mutation within the SET domain of *Ezh2* that generates a hypomorph that is
93 predominately defective in tri-methylation. We also analyzed cells treated with a small
94 molecule inhibitor that blocks tri-methylation more efficiently than di-methylation. The
95 expression level of PRC2 has known effects on gene regulation, so we used strategies that do
96 not impact the protein level or complex integrity, thus allowing a focus on methyltransferase
97 activity. There are multiple small molecules that interrupt PRC2 methyltransferase activity both
98 for research and current clinical trials; we used GSK343 (Bradley et al., 2014; Fraineau et al.,
99 2017; Liu et al., 2015; Xu et al., 2019; Yang et al., 2019). Mutations in the catalytic SET domain
100 of *Ezh2* have been identified from a variety of cancers; we created cell lines containing one of
101 the inactivating mutations for our experiments (Antonysamy et al., 2013). We found that this
102 mutation had a strong impact on H3K27me3 levels, but not on H3K27me2 levels. When these
103 cells were differentiated in an undirected fashion they did not show the significant visual
104 phenotypes seen with *Ezh2* knockout cells. While expression of some genes was altered, there
105 were a number of PRC2 target genes that did not rely upon H3K27me3 for their regulation. The
106 most dramatic phenotype observed was when cells were challenged to maintain their
107 differentiated identity. Inhibitor treated and point mutated cells reverted readily to an ES
108 phenotype when placed back into conditions that support ES cell growth. Thus, H3K27me3 was
109 required for cells to maintain their identity rather than for the initial differentiation.
110
111 **Results**
112 PRC2 catalyzes di- and tri-methylation of histone H3 and is associated with gene
113 repression. Previous studies have shown that deletion of PRC2 components in mouse ES cells
114 has minimal effects on the undifferentiated, self-renewing state (Juan et al., 2016; Lavarone et
115 al., 2019; Shen et al., 2008; Wassef et al., 2019). Yet deletion of EZH2, the catalytic subunit of
116 PRC2, results in cells that do not differentiate and embryos that are reabsorbed by day E10.5

117 (Pasini et al., 2004). However, the requirements for specific methylation functions of PRC2 in
118 differentiation and in the accompanying changes in gene expression have not been explored in
119 detail. We examined the role for H3K27me3 in regulation by looking at stochastic
120 differentiation of ES cells into embryoid bodies. Embryoid body (EB) formation is a well-studied
121 method of undirected differentiation with predictable changes in gene expression (Fig 1A and
122 (Behringer et al., 2016; Dang et al., 2002). Cells where PRC2 core components haven been
123 deleted fail to form normal embryoid bodies, presumably because the cells apoptose when
124 pushed to differentiate(Chamberlain et al., 2008). Since PRC2 has been shown to play
125 regulatory roles independent of H3K27 tri-methylation, including H3K27 di-methylation and
126 proposed non-methyltrtansferase functions, the requirement for the H3K27me3 modification
127 at individual genes during differentiation as well as its role in maintaining cell identity remains
128 unclear (Ahmed et al., 2018; Ai et al., 2017; Pereira et al., 2010).
129
130 **Inhibiting methyltransferase activity with the small molecule GSK343 does not block**
131 **differentiation potential**
132
133 As a starting point to understand the role of H3K27 methylation by PRC2 during ES cell
134 differentiation, we treated cells with the small molecule inhibitor GSK343 which blocks the
135 methyltransferase activity of EZH2 (Fioravanti et al., 2018; Lue & Amengual, 2018; Yang et al.,
136 2019). Treatment with DMSO was used as a control (Fig 1B). Unlike PRC2 knockouts, GSK343
137 treated cells form embryoid bodies that have a similar morphology to their DMSO treated
138 counterparts (Fig 1C.) Embryoid bodies formed after either DMSO or GSK343 treatment are
139 phenotypically similar to those made by WT cells. In contrast, PRC2 knockout cells tested in
140 parallel failed to form embryoid bodies ((Lavarone et al., 2019) and Fig. 2E). Thus, the inhibition
141 of methyltransferase activity can be phenotypically separated from PRC2 knockout cells.
142
143 To determine the molecular phenotype of blocking methyltransferase activity, we
144 performed RNA-seq experiments to compare changes in gene expression between cells treated
145 with the inhibitor and control over the differentiation time course. Gene expression was largely

146 similar between the two treatments especially in early stages of differentiation (Supp. Fig. 1).
147 We then examined known PRC2 target genes and found examples of genes whose expression
148 pattern across differentiation was the same in DMSO and GSK343 treated cells (e.g. Tbx3 or
149 Sox3, Fig. 1D) as well as genes whose expression was altered in GSK343 treated cells (e.g., Wnt3
150 and Itgb7, Fig 1D). The trends observed with these two classes of genes were found to be
151 mirrored in the full complement of PRC2 targets. We classified PRC2 target genes into two sets,
152 those that required H3K27me3 for their regulation and those that do not need this modification
153 to preserve normal gene expression patterns during embryoid body formation. Genes were
154 defined as independent of the H3K27me3 modification if their expression remained within 1.2
155 fold of the WT expression at all time points (Fig 1E). We conclude that inhibiting the
156 methylation activity of PRC2 alters gene expression at a subset of targets but does not block
157 differentiation the way knockouts of the complex do.
158
159 **Point mutation to the SET domain inhibits methyltransferase activity**
160
161 We sought to extend and refine the findings made using GSK343 by generating a
162 hypomorphic mutation in *Ezh2* that had a defined impact on H3K27 methylation. We generated
163 mutant cells that allowed us to examine the contribution of H3K27 tri-methylation to gene
164 regulation and differentiation during EB formation. Inactivating point mutations in the SET
165 domain of EZH2 have been identified in several human cancers. We chose one of those
166 mutations, human R635C, which is analogous to mouse R681C, for analysis in mouse cells. This
167 residue is conserved across methyltransferases and located in a region that is important for
168 coordinating the methyl donor (Fig 2A and (Antonysamy et al., 2013). We used a baculoviral
169 system to reconstitute WT and mutant PRC2. We confirmed that this residue is important for
170 tri-methylation of H3K27 by PRC2 using an in vitro methyltransferase assay. We compared it to
171 WT EZH2 and another SET domain mutation (Y722D) that has been previously shown to block
172 methylation (Lavarone et al., 2019), Fig 2B). The complexes that contained WT EZH2
173 methylated both core histones and purified H3 in a time and concentration dependent manner
174 (Supp. Fig. 2). In contrast, mutant complexes show drastically reduced levels of activity. Using

175 two separate purifications, residual activity of the mutant complex was always under 2% of the
176 purified WT complexes (Fig. 2B and Supp. Fig. 2). This was not due to a failure of the mutant
177 EZH2 to incorporate into a stable complex as all core components were pulled down with a flag-
178 tagged SUZ12 (Supp. Fig. 2E). We conclude that the *Ezh2* 681C mutation reduces the
179 methyltransferase activity of the complex by at least 50-fold.
180
181 We introduced the R681C mutation into the CJ7 mouse ES cell line using the CRISPR-
182 Cas9 system. We isolated two independent with this homozygous point mutation in the
183 endogenous *Ezh2* gene (called CJ7 Ezh2$^{681C-99}$ and CJ7 Ezh2$^{681C-102}$). The phenotypes that we
184 describe below were consistent between these two independent clones.
185
186 We determined whether the point mutation would lead to significant reduction of
187 H3K27me3 in cells as anticipated from the enzymatic defect seen in vitro. Lysine residues can
188 be mono, di or tri-methylated. Mono-methylation is spread broadly throughout the genome
189 and di-methylation is loosely linked with repressed genes, though this is poorly defined in most
190 cell types. Tri-methylation of H3K27 is closely associated with repressed genes, presumably due
191 to binding of the CBX family of proteins contained in the PRC1 complex to K27me3 and
192 subsequent repression by this family of complexes (Bernstein et al., 2006). We performed
193 western blots on whole cell lysates from WT, knockout and the point mutant cells and probed
194 them with antibodies to di- and tri- H3K27 methylation and EZH2 (Fig 2C and Supp. Fig. 3).
195 H3K27me3 was reduced to levels we could not detect in the mutant cells, as was seen in the
196 knockout cells, but the levels of di-methylation were largely unaffected in the R681C mutant
197 cells.
198
199 The mutant ES cells look phenotypically similar to WT cells and self-renew (Fig 2D). This
200 was the anticipated result since knockout cells in the PRC2 core components EZH2 and EED are
201 also phenotypically similar to WT cells and can self-renew. We examined whether the mutant
202 cell lines would form embryoid bodies similar to those formed by WT cells, would apoptose like
203 *Ezh2* or *Eed* knockout cells, or would take an alternate path. We formed embryoid bodies by

204 the hanging drop procedure and compared the resultant phenotypes of WT, the point mutant
205 and knockout cells. We found that the mutant cells formed embryoid bodies, making them
206 phenotypically separate from the knockout cells (Fig 2D). This revealed that the dramatic
207 reduction in H3K27me3 we see in the point mutant cells does not stop the cells from
208 differentiating, at least at a gross level.
209
210 We determined whether the mutant PRC2 complex was localized to the same genomic
211 regions as the WT complex by characterizing peaks of the core PRC2 component SUZ12 through
212 use of CUT&RUN. There were fewer peaks of PRC2 chromatin binding in the mutant cells when
213 compared to WT, as expected due to the lack of H3K27me3 which facilitates binding and
214 spreading of PRC2 (Oksuz et al., 2018). There was a high degree of overlap between peaks of
215 occupancy in ES cells (Fig. 2E). We also observed overlap in binding of SUZ12 between WT and
216 mutant cells at Day 4 and Day 8 of differentiation into embryoid bodies (Fig. 2F). We conclude
217 that in these cells the major effect of the point mutation was to reduce the tri-methylation of
218 H3K27. This is similar to the results found in other studies of *Ezh2* point mutations (Lavarone et
219 al., 2019).
220
221 To further test the developmental potential of the 681C mutant embryonic stem cells
222 we assessed the formation of beating clusters of cardiac cells. For this assay cells are
223 differentiated in hanging drops and then plated in individual wells to form a monolayer in
224 differentiation media. After 10-15 days of differentiation each well is visually examined for the
225 presence of pulsing cells. Beating clusters formed from both WT and mutant cells. There was
226 some variation in the proportion of EBs that could form beating clusters between the two 681C
227 mutant strains, but in all cases the mutant cells could form beating clusters (Fig. 2G). These data
228 bolster the conclusion that the reduction in H3K27me3 does not prevent cells from
229 differentiating. The R681C mutation therefore offers an opportunity to examine the
230 contribution of tri-methylated H3K27 to gene regulation during differentiation and raised the
231 issue of whether molecular changes are caused by the point mutation.
232

233 **Molecular phenotype of *Ezh2* point mutant cells**

234

235 To determine whether there were molecular phenotypes associated with the
236 hypomorphic mutation of *Ezh2*, and the resultant loss of H3K27me3, we determined the target
237 genes of PRC2 in our cell lines and measured their gene expression levels. To annotate target
238 genes in this system, we performed CUT&RUN analysis using antibodies to H3K27me3, RING1b,
239 EZH2 and SUZ12 in WT cells as embryonic stem cells (ESC) and as Embryoid bodies after
240 differentiation for eight days (D8EB). Target genes were defined as having a broad peak of
241 H3K27me3 over the transcription start site in at least two time points. There have only been a
242 small number of studies of PRC2 localization in differentiating cells, but of the approximately
243 seven thousand target genes we identified, just over 70% overlapped with previously published
244 data (Fig. 3A and (Juan et al., 2016)). We note that peaks called from our data set that did not
245 overlap with previous called peaks showed signal in the published data that was below the
246 threshold, indicating further agreement between the analysis done here and previous work.
247 There were far more targets called using the H3K27me3 than with the individual components of
248 either polycomb complex, though the targets are largely overlapping (Fig. 3B). This is likely due
249 to differences in the strength of individual antibodies. Therefore, we used the targets identified
250 with H3K27me3 for further analysis. In keeping with the western blot from whole cell lysates,
251 H3K27me3 was reduced on target genes in mutant cells (Fig. 3C). Levels of H3K27me3 were
252 significantly lower in mutant cells at day 4 of differentiation and then were increased at day 8
253 of differentiation but to levels well below WT levels. The residual tri-methylation at day 8 might
254 be due to EZH1 function (Lavarone et al., 2019; Margueron et al., 2008; Shen et al., 2008). We
255 focus below on the events that happen during these first four days of differentiation and the
256 impact of the lack of H3K27me3 during this time frame. We conclude that the ability of the
257 mutant cells to differentiate was not due to retention of normal tri-methylation levels
258 specifically on target genes.

259

260 The experiments described above using small molecule inhibitors revealed that there
261 are genes that require H3K27me3 for their regulation and those that do not require H3K27me3

262 to maintain proper regulation. We investigated whether the point mutant cells showed these
263 same two gene classes. We performed RNA-seq analysis from ES cells and both D4 and D8EBs
264 from WT, CJ7 Ezh2$^{681C-99}$ and CJ7 Ezh2$^{681C-102}$ cells. The data for both mutant cell lines are nearly
265 overlapping and so for clarity we present the data from the CJ7 Ezh2$^{681C-99}$ (Supp. Fig. 4). For
266 this analysis we defined PRC2 target genes as those that had a statistically significant peak of
267 H3K27me3 from CUT&RUN data at either D4 or D8 during the EB formation protocol. PRC2
268 target genes were identified using wild-type H3K27me3 peaks called by Homer using a p-value
269 threshold of 0.001, a length of at least 1500 bp, 1rpkm in at least two time points and signal
270 overlapping Refseq annotated genes (TSS+-5kb). As with the cells treated with the small
271 molecule inhibitor, we could separate genes that rely on H3K27me3 from those that do not
272 need a high level of the modification for their regulation (Fig 3D). The gene expression patterns
273 from the mutant cells and from the GSK343 treated cells clustered based upon day of
274 differentiation rather than by whether they were drug treated or mutant (Supp. Fig. 5),
275 although the correlation was not as strong between drug treated cells and mutant cells as that
276 seen between the two mutant cell lines. We detected both activated and repressed genes that
277 fell into methyltransferase-dependent and –independent categories. The 350 genes that are
278 normally repressed during differentiation in WT cells, and were either similarly repressed or
279 were not repressed in mutant cells, showed more consistent patterns than the genes that were
280 normally activated in WT cells. These patterns were well established by D4 of differentiation,
281 thus we used repressed genes to further analyze any characteristics specific to the
282 methyltransferase dependent or to the independent genes.
283
284 We examined whether the level of H3K27me3 normally found on the genes in WT cells
285 or the amount of signal remaining in the mutant cells could predict whether a gene would be
286 dependent on the modification for its regulation. However, there was not a difference in the
287 levels of tri-methylation based on whether the genes require this modification for their
288 regulation (Fig. 3E). There was also strong overlap in the genes with PRC2 peaks suggesting that
289 the complex was still targeted normally (Supp. Fig 6) We then examined several characteristics
290 of 350 genes that are normally repressed during differentiation of WT ES cells including other

291 histone modifications, CpG methylation, and further sub dividing genes by their dependence on
292 H3K27me3 (Supp. Fig. 6). None of these characteristics showed any significant differences
293 between genes who repression was dependent upon methyltransferase activity and genes
294 whose repression was not dependent on methyltransferase activity. We conclude that there is
295 a variable reliance on H3K27me3 for gene regulation and that H3K27me3 is not the only driver
296 of PRC2 target gene repression during EB formation, just as full levels are not needed for
297 differentiation.
298
299 **Methyltransferase point mutants cannot maintain differentiated cell identity**
300
301 A major issue in developmental gene expression concerns the interplay between
302 establishment and maintenance of gene expression profiles during differentiation. The
303 Polycomb group (PcG) system, including PRC2, plays a role in both aspects of gene regulation in
304 flies and in mammals. Substantial early work on mutant Drosophila highlighted a role for the
305 PcG, including gene products now known to compose PRC2, in maintenance. Given that we saw
306 limited impact of the ablation of H3K27me3 on establishment of the differentiated EB
307 phenotype, we tested whether the mutant or drug treated mouse cells were able to maintain a
308 differentiated state.
309
310 Under normal conditions, cells differentiated into embryoid bodies cannot revert to
311 ESCs without major manipulation such as introducing Yamanaka transcription factors
312 (Nakagawa et al., 2008; Takahashi & Yamanaka, 2006). To determine if the 681C point mutant
313 cells stably committed to a differentiated state, we formed day 8 EBs with WT and mutant cells,
314 dissociated the embryoid bodies into single cells and re-plated them in ESC conditions without
315 any additional manipulation. The cells were cultured in the ESC media for five days and then
316 stained for alkaline phosphatase (AP) activity. After incubation with an appropriate
317 colorometric substrate, ESCs become bright pink due to their alkaline phosphatase activity,
318 while feeder cells or any other differentiated cells remain unstained. We found a ten-fold
319 increase in the number of AP-positive colonies generated by the mutant cells over the WT (Fig.

320 4A and 4B). We asked whether this lack of commitment was maintained after longer periods of
321 differentiation and found that after 14 days there remained more cells that could revert to ES
322 cells, but to a considerably lesser extent than seen after 8 days (Figs. 4A, 4B). We conclude that
323 the mutant cells are not stably committed to the more defined lineages but can switch back to
324 an undifferentiated state, but that this flexibility decreases after two weeks of differentiation.
325
326 We used the small molecule inhibitor GSK343 to examine the time period during which
327 this flexibility is established. There were three possibilities: a) full levels of H3K27me3 might be
328 needed continuously to maintain the differentiated state; b) they might be needed at specific
329 times as the cells are differentiating; c) they might be needed only when cells are challenged
330 with external stimuli that allow reversion to embryonic stem cells. Examination of the mutant
331 cells addressed blocking full levels of methylation throughout the experimental time course,
332 but did not address the time period when that lack of activity was most important. To separate
333 the possibilities, we added or removed GSK343 during the differentiation time-course (Fig. 5A
334 shows the experimental design). To mimic the WT and point mutant conditions a subset of cells
335 were treated continuously with DMSO or GSK343 respectively. These treatments served as both
336 a baseline for altered times of GSK343 application. They also served to validate that the results
337 observed with re-plating of mutant cells were not caused by off target effects of the CRISPR
338 genetic manipulation or by mutations acquired during selection of these cells. Cells
339 continuously treated with GSK343 had higher numbers of AP-positive cells following re-plating
340 at 8 days, similar to the mutant cells; in contrast to the mutant cells there even more AP-
341 positive cells following re-plating after 14 days of differentiation in GSK343. GSK343 treatment
342 affects both di- and tri-methylation which might account for the increased plasticity seen at
343 later time points in drug treated cells (Supp. Fig. 7).
344
345 In addition to continual treatment with inhibitor, we varied the timing of GSK343
346 addition as depicted in Fig. 5A. Briefly, we treated ES cells for three days with either DMSO or
347 GSK343 before starting the differentiation. When embryoid body formation was initiated or at
348 day 4 of differentiation we changed the treatment from DMSO to GSK343 (or vice versa) for

349 half of the cells. We also switched the treatment at the time of re-plating into the ES conditions
350 at day 8. Finally, we allowed cells to differentiate to day 14 and switched treatment regimen
351 (Fig. 5A). The treatment type was switched just once in each scheme so we could determine
352 whether blocking the methylation of H3K27 at early or later stages of differentiation had the
353 greatest effect. These experiments allow us to determine whether reducing H3K27me3 has the
354 greatest effect on cell identity when the cells are differentiating, when they are challenged by
355 re-plating or throughout the differentiating time-course.
356
357 We found that the crucial window for treatment with the inhibitor was in the first four
358 days of embryoid body formation (Fig. 5A, B, C). Increased staining by alkaline phosphatase
359 activity was seen in all cells that had initially been treated with inhibitor, regardless of when it
360 was removed (Fig. 5C). Notably, treating with GSK343 for three days prior to inducing
361 differentiation, then removing the inhibitor when differentiation was initiated, led to a
362 significant increase in ES cells following re-plating at day 8. The only case where we saw
363 increased staining in re-plated cells that were initially treated with DMSO was when the
364 inhibitor was added at the onset of differentiation (Fig 5B, C). We conclude that the inhibition
365 of methyltransferase activity either immediately prior to differentiation or during the first four
366 days of differentiation allows the cells to remain in a more plastic state such that they can
367 revert to a stem cell-like phenotype when placed in the proper growth conditions.
368
369 When we examined the ability of treated cells to form beating colonies after treatment
370 with the small molecule we found no difference in the proportion of colonies that
371 spontaneously start beating between any of the treatment groups (Fig. 5D). This is consistent
372 with the data from the point mutant cells where both WT and mutant cells could form beating
373 colonies and further indicates that there is no deficit in the ability of the cells to differentiate
374 when H3K27 methylation is inhibited. Thus, as was seen with the comparison of WT and point
375 mutant cells, the obvious difference between DMSO and small molecule treated cells occurred
376 when cells were challenged to grow in the ESC culture conditions (Figs 5B,C). We conclude that
377 H3K27me3 methylation is more important in maintaining the differentiated state than in

378 generating that state, and that the critical time window occurs early in the differentiation
379 process.
380
381 The GSK343 treated cells and the mutant cells both appeared to revert to a pluripotent
382 state. To verify that these cells retained developmental potential we re-differentiated these
383 cells and determined whether they display the characteristic ability of ES cells to develop more
384 committed cells. We used the re-plated cells from both 681C mutant cells and those treated
385 with the inhibitor and attempted to make embryoid bodies. Both sets of re-plated cells were
386 able to make embryoid bodies, which confirms that they have developmental potential (Data
387 not shown).
388
389 To examine whether the reversion to a pluripotent state involved substantive changes in
390 gene expression, as opposed to gene expression changes in a few key genes, we examined
391 genome-wide gene expression pattern of the reverted cells and compared those to ESCs. To
392 examine the molecular phenotype of the re-plated cells, we isolated and sequenced RNA from
393 drug treated day 14 cells that were re-plated and had reverted to ES cell phenotype.
394 Unsupervised clustering showed that the average expression profiles of the cells that had been
395 treated with GSK343, and therefore had much higher levels of reversion, were more like WT ES
396 cells than to the DMSO treated and re-plated control cells (Fig. 5E.) We conclude that the cells
397 we see staining with alkaline phosphatase in our re-plating assays are reverting to an ES
398 phenotype. We examined the subset of PRC2 target genes that are normally repressed during
399 differentiation and found that many are reactivated when cells treated with GSK343 are re-
400 plated. This differs from the genes that are reactivated in the cells initially treated with DMSO.
401 The changes in gene expression observed following re-plating of cells treated with GSK343 were
402 significantly different from the patterns observed after re-plating of cells treated with DMSO.
403 (Supp. Fig. 7C). These expression pattern changes show the same response to the time of
404 treatment with GSK343 as seen above; reversion to the WT pattern requires GSK343 treatment
405 early in differentiation. From these data, we conclude that though all cells are placed under
406 developmental stress when re-plated into ES conditions, only those where H3K27 methylation

407 has been blocked revert to an ES cell phenotype. This underlines the importance of K3K27me3
408 in establishing the heritable gene expression profile of differentiated lineages.
409
410 **Discussion**
411
412 These studies offer two advances in understanding the role for tri-methylation of H3K27
413 during differentiation of ES cells into embryoid bodies. First, many PRC2 targets continue to be
414 regulated in a normal manner during the first four days of differentiation despite significantly
415 reduced H3K27me3 levels on these targets (Fig. 3.) Thus, H3K27me3 is not necessary for
416 repression of a significant set of PRC2 targets, indicating compensating mechanisms for
417 repression of these genes. Second, while many PRC2 targets are dysregulated when H3K27me3
418 is blocked, we did not observe a significant impact on differentiation. In contrast, there was a
419 large enhancement of the ability of differentiated cells to revert to a pluripotent phenotype
420 when placed into embryonic stem cell culture conditions. We conclude that the primary role for
421 H3K27me3 during early differentiation is maintenance of the differentiated state.
422
423 Differentiated WT cells are not generally capable of reverting to an ES phenotype when
424 their growth conditions are altered by a change in media. In normal cases, it takes the
425 reactivation of key transcription factors to allow cells to return to that state. In contrast, *Ezh2*
426 point mutant cells and those that that have been treated with a small molecule inhibitor readily
427 revert to an ES phenotype when placed into media that supports that type of growth. This was
428 seen at both the cellular and molecular level. When we varied the time windows where
429 inhibitor was present, we found that the crucial window for normal H3K27me3 levels was
430 between the start of differentiation through the first four days of embryoid body formation.
431 Not having the ability to add the tri-methylation modification at those early stages of
432 differentiation sets the stage for the cells to be able to revert to an ES phenotype when
433 challenged, even if H3K27me3 is restored later during embryoid body formation. In the setting
434 of the early stages of ES differentiation into embryoid bodies, the H3K27me3 modification is
435 acting analogously to a stopper on a swinging door. When the modification is present the door

436 will only open one way and the cells cannot go backward, but removal of the modification
437 enables the door to swing both ways allowing cells to go back and forth between the
438 differentiated and pluripotent state in response to external signals.
439
440 There are potential implications for these data in terms of the use of small molecule
441 inhibitors in therapeutic situations. Multiple adult cell types have different requirements for
442 PRC2 during their differentiation. Most relevant to the inhibition of PRC2 is the development of
443 blood cells. PRC2 is required for the differentiation of blood stem cells and is the site of some of
444 the highest levels of PRC2 expression in healthy adult tissues. If the phenotypes that we have
445 observed during embryoid body formation occur in a similar manner in blood stem cells,
446 treating patients with the small molecule inhibitors might alter the stability of commitment of
447 healthy stem cells, raising the possibility of novel cancers arising from cells that cannot stably
448 differentiate. Indeed, at least one clinical trial was temporarily suspended because patients had
449 developed novel cancers (Fioravanti et al., 2018; Harris, 2018; Italiano et al., 2018). Determining
450 the effect of blocking H3K27me3 in other differentiating cell lineages might be important to
451 clinical intervention by expanding the knowledge of the potential side effects.
452
453 We note that it is difficult to completely eliminate H3K27 methylation with mutations
454 (Lavarone et al., 2019), and that the mutation we generated in *Ezh2* specifically impacts
455 H3K27me3, especially early in differentiation, but does not eliminate all methylation of H3K27.
456 This is both a limitation and an advantage; the significant impact on H3K27me3 early in
457 differentiation allowed us to show that loss of tri-methylation has a potent phenotype
458 (unstable commitment) at this stage yet does not have a discernible differentiation phenotype.
459 These data demonstrate a striking difference in the dependency of these two key phenotypes
460 on H3K27me3. This *Ezh2* mutation also has a molecular phenotype when gene regulation is
461 examined, raising the possibility that the network of genes that require H3K27me3 for
462 appropriate regulation at this stage are primarily responsible for driving stable commitment to
463 the differentiated state.
464

465

466 Methods

467 **Cell Culture**

468 ES cells: CJ7 WT, CJ7 *Ezh2*-/- and CJ7 *Eed*-/- cells were a generous gift from the laboratory of
469 Stuart Orkin. We cultured all embryonic stem cells on a monolayer of feeder MEFs in ES media
470 (DMEM (Gibco 11995-506) supplemented with 20%FBS, NEAA, pen/strep, glutamax, and LIF) on
471 tissue culture treated flasks coated with 0.2% geletin. Media was changed daily and cells were
472 split every 2-3 days.

473

474 EZH2 point mutant Cells: Point mutations were introduced into CJ7 WT using CRISPR RNP
475 transfected into cells with the Amaxa mouse ES kit (Lonza VPH-1001). $1x10^6$ cells were
476 transfected with the RNP containing two separate guide RNAs a single stranded donor oligo and
477 a linearized puromycin resistance gene. Cells were plated into three wells of a six well plate
478 with puroR MEFs and regular ES media. The next day puromycin was added to the wells in a
479 range of concentrations and kept on the cells for the next two days. Following selection,
480 resistant cells were expanded, individual colonies were then re-plated into twenty-four well
481 plates and checked for the presence of the mutation by restriction enzyme digestion followed
482 by confirmation with sequencing.

483

484 EB formation: Embryoid bodies were formed using the hanging drop method(Behringer et al.,
485 2016; Dang et al., 2002). Briefly, ES cells were trypsinized, de-MEFed and then resuspended in
486 differentiation media (IMDM (Gibco 12440-053) supplemented with 20% FBS, pen/strep, and
487 glutamax. No LIF). Droplets containing approximately 180 cells were incubated for four days so
488 that spheres of differentiating cells could form. After the four days EBs were collected and
489 grown in suspension in non-adherent plates or used for subsequent experiments.

490

491 Beating heart assay: Beating clusters were differentiated from day 4 embryoid bodies (Boheler
492 et al., 2002; Hescheler et al., 1997). Individual EBs were transferred into individual wells of a
493 gelatinized 12 well plate. Cells were maintained in differentiation media throughout the

494 experiment. Wells were monitored for beating colonies for the next 15 days and were scored as
495 positive if there were any beating cells in that time period.
496
497 **Western Blot**
498 The antibodies that were used probe the Western blots were from Cell Signaling Technology
499 H3K27me3 (9733S) and H3K27me2 (9728S) as well as from EMD Millipore EZH2 (07-689).
500
501 **RNA-seq**
502 RNA was isolated from whole cells using the Nucleospin RNA kit from Macherey Nagel
503 (740955.50). We then depleted rRNA using the Ribozero Gold kit from Epicentre (RZG1224).
504 cDNA was synthesized from the purified RNA using the Superscript Vilo cDNA sequencing kit
505 from ThermoFisher (11754050) the libraries were assembled as previously described (Bowman
506 et al., 2013). Three replicates were completed for all experimental conditions except the Day 14
507 re-plated cells where two replicates were completed.
508
509 **Methyltransferase Assay**
510 Purified protein complexes were incubated at room temperature with a histone substrate at a
511 final concentration of 500nM and approximately 500nM radioactive SAM (Adenosyl-L-
512 methionine S-methyl^{3}H from PerkinElmer (NET155H250UC)) in methyltransferase buffer (10%
513 glycerol, 25mM HEPES PH 7.9, 2mM MgCl with 1mM DTT added fresh). Unless otherwise
514 specified all reactions ran for one hour before being stopped with the addition of 6x SDS buffer.
515 Samples were then run on an SDS page gel, coomassie stained and incubated in AMPLIFY
516 Amersham/GE (NAMP100) for 20 minutes. The gel was dried and exposed to film for a
517 minimum of 24 hours before developing.
518
519 **Protein purification**
520 The ORF for each member of the core PRC2 complex were cloned into the pFastBac1
521 baculovirus with Suz12 tagged with 3xFlag. Sf9 transfection with bacmid DNA and virus
522 amplification were performed essentially as described for the Bac-to-Bac Baculovirus
523 Expression System (ThermoFisher Scientific). Sf9 cells were maintained in Hyclone CCM3

524 (CCM3 liquid medium with L-glutamine, GE Healthcare Life Sciences SH30065.02)
525 supplemented with 50 U/ml Penicillin-Streptomycin (ThermoFisher Scientific, 15140-122). For
526 protein expression, $2x10^6$ Sf9 cells/ml were infected at an MOI of approximately 10. Cells were
527 harvested 66 hours post infection by centrifugation at 5000xG for 15 minutes. Cells were lysed,
528 treated with DNAse1 then the complex was bound to M2 and the complex was eluted with flag
529 peptide.
530
531 **CUT&RUN**
532 CUT&RUN experiments were performed as described (Skene & Henikoff, 2017). The antibodies
533 we used were from Cell Signaling Technology H3K27me3 (9733S), EZH2 (5246S), SUZ12 (3737S)
534 and Bethyl laboratories RING1b (A302-869A). Libraries were constructed as described in the
535 RNA-seq section. Two replicates were completed and representative experiments are shown.
536
537 **Alkaline Phosphotase Assay**
538 Cells were stained according to the instructions in the Stemgent AP Staining Kit II from
539 Reprocell (00-0055). Images of stained wells were quantified using ImageJ FIJI software.
540
541 **Bioinformatics Methods**
542
543 RNA-seq data processing: All RNA sequencing reads were aligned to the mm10 genome using
544 STAR v2.5.3 (Dobin et al., 2013). Gene annotations were obtained from Ensembl (Hunt et al.,
545 2018) Genome browser tracks were generated using Homer v4.10.3 (Heinz et al., 2010) and
546 visualized in IGV (Robinson et al., 2011). Reads in exons of Refseq annotated genes were
547 counted using featureCounts v1.6.1(Liao et al., 2014). edgeR (Robinson et al., 2010) was used to
548 normalize reads and calculate FDR using triplicates. All further calculations and figures were
549 made using R v3.3.2 (Dessau & Pipper, 2008). For all heatmaps, standard z-scores calculations
550 were made using average RPKMs of triplicates for each gene across all conditions. Genes were
551 narrowed down to only PRC2 targets using H3K27me3 CUT&RUN data. Only genes changing in
552 untreated or wild-type cells over the time-course were used for further analysis. The genes

553 were filtered using cut-offs of at least 0.5 RPKM average expression at any timepoint, at least
554 1.5 fold-change and maximum 0.05 FDR while comparing Day 8 and Day 4 or Day 4 and Day 0.
555 Genes were then clustered based on up or down-regulation in control cells and up or down-
556 regulation or unchanged gene expression in mutant or treated cells.
557
558 For Fig. 5E, unsupervised clustering was performed using R's heatmap.2 function. CpG and GC
559 levels were calculated using Homer's annotatePeaks function.
560
561 CUT&RUN data processing: All CUT&RUN reads were aligned to the mm10 genome using
562 bowtie2 and filtered using samtools (Li et al., 2009) to keep uniquely aligned reads. Genome
563 browser tracks were generated using Homer v4.10.3 and visualized in IGV. Peaks were called
564 using Homer's findPeaks function for broad peaks. PRC2 target genes were identified using
565 wild-type H3K27me3 peaks at least 1500 bp in length, 1rpkm in at least two time points and
566 overlapping Refseq annotated genes (TSS+-5kb). Target genes for Suz12 and Ezh2 were
567 identified using the same parameters as H3K27me3. Average of RPKMs of two replicates was
568 calculated for Suz12 CUT&RUN data, and target genes were identified using the same
569 parameters as H3K27me3. For Figures 2E and 2F, average of RPKMs of two replicates was used
570 to find Suz12 peaks. For Figure 2F, peaks from D4 and D8 were merged. Deeptools
571 v3.3.0(Ramírez et al., 2014) was used to make average profile plots for Fig. 3E.
572
573 Published ChIP-seq data sources and processing: Published data for other canonical and non-
574 canonical PRC2 components was downloaded from GEO as follows : H3K27me3 (GSM2282188,
575 GSM2282191, GSM2282192) (Juan et al., 2016), EPOP (GSM2098943) (Beringer et al., 2016),
576 Jarid2 (GSM491760) (Li et al., 2010), H3K4me1 (GSM1180178), H3K4me3 (GSM1180179),
577 H3K9me3 (GSM1180180), H3K36me3 (GSM1180183) (Hon et al., 2014). FASTQ files were
578 downloaded from GEO using sratools v2.9.1 (https://ncbi.github.io/sra-tools/). All reads were
579 aligned to the mm10 genome using bowtie2 and filtered using samtools to keep uniquely
580 aligned reads. Genome browser tracks were generated using Homer v4.10.3. Deeptools v3.3.0
581 was used to make average profile plots for Fig. 3C and E.

582

583

Figure 1.

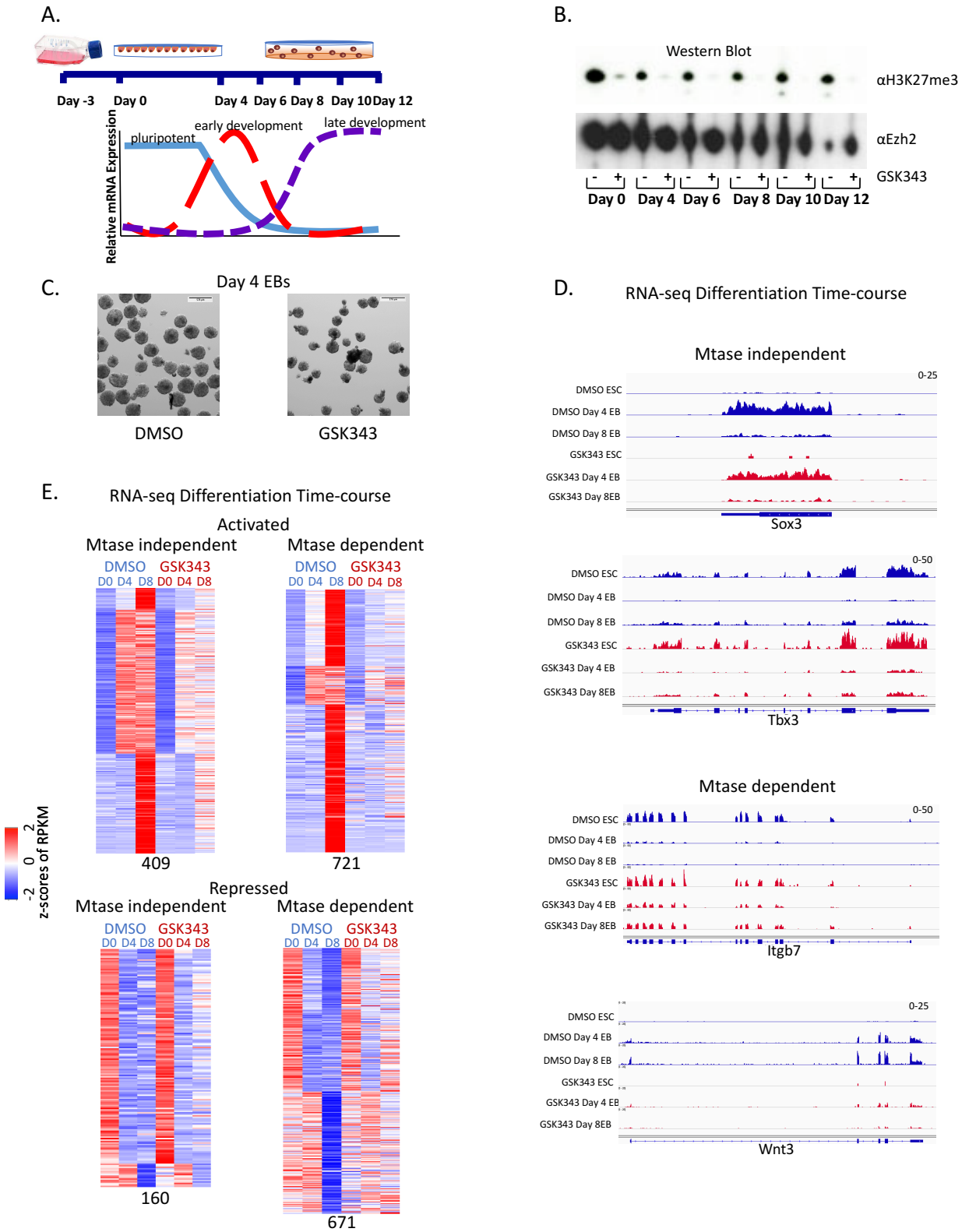
A.
Day -3
Day 0
Day 4
Day 6
Day 8
Day 10
Day 12
Relative mRNA Expression
pluripotent
early development
late development
B.
Western Blot
αH3K27me3
αEzh2
GSK343
Day 0
Day 4
Day 6
Day 8
Day 10
Day 12
C.
Day 4 EBs
DMSO
GSK343
D.
RNA-seq Differentiation Time-course
Mtase independent
DMSO ESC
DMSO Day 4 EB
DMSO Day 8 EB
GSK343 ESC
GSK343 Day 4 EB
GSK343 Day 8EB
Sox3
Tbx3
Mtase dependent
Itgb7
Wnt3
E.
RNA-seq Differentiation Time-course
Activated
Mtase independent
Mtase dependent
DMSO
GSK343
D0 D4 D8 D0 D4 D8
409
721
Repressed
160
671
z-scores of RPKM

584

585

Figure 2.

A.

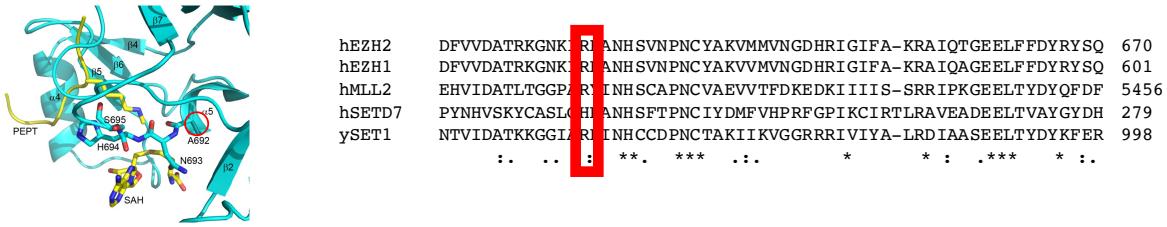

B.

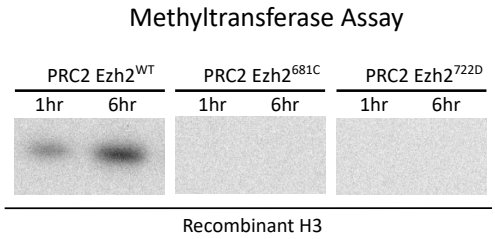

C.

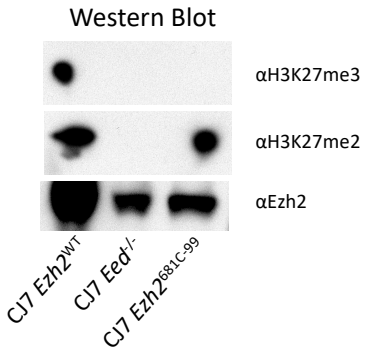

D.

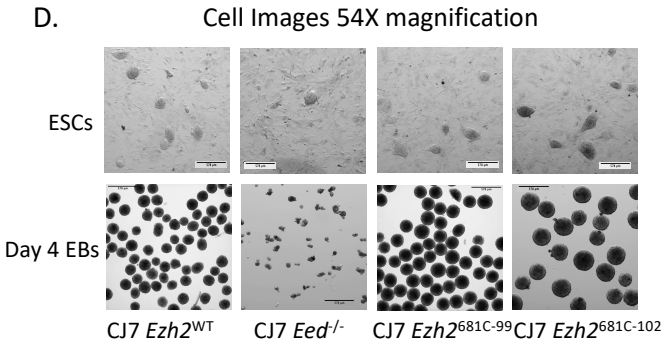

E.

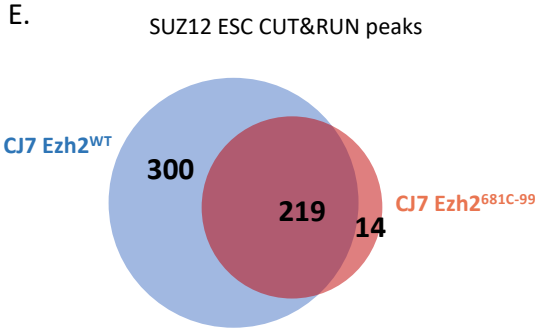

F.

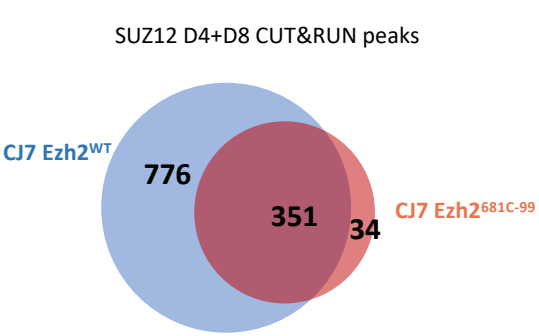

G.

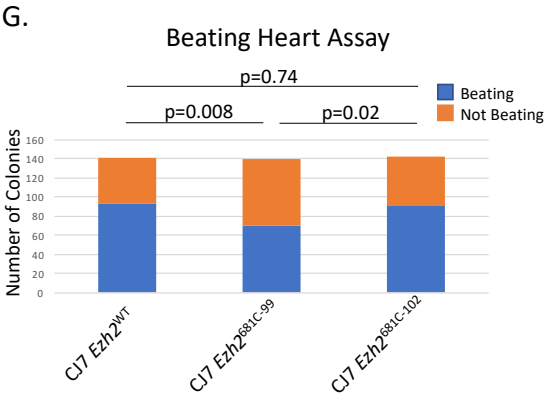

586

Figure 3.

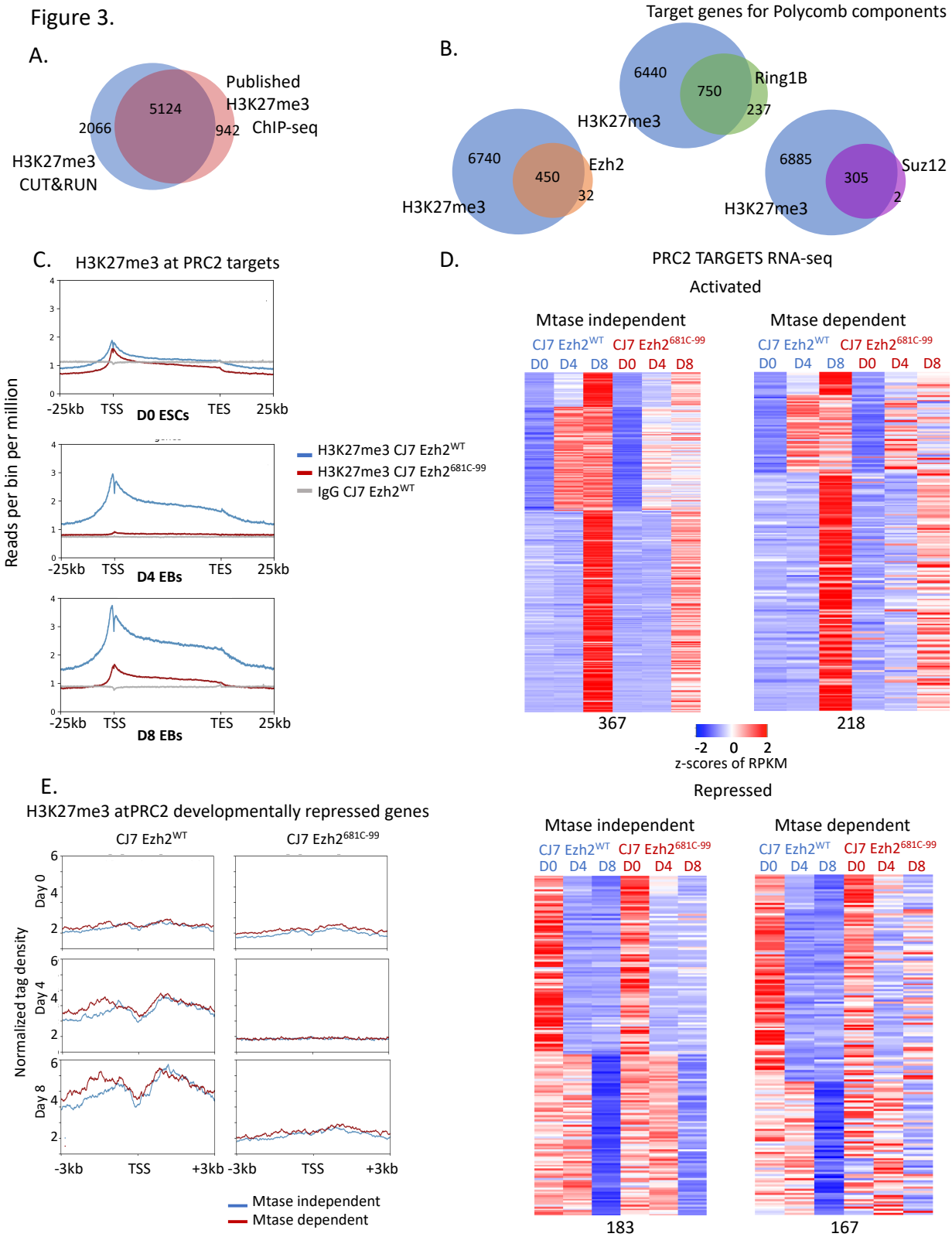
A.
Published H3K27me3 ChIP-seq
5124
2066
942
H3K27me3 CUT&RUN
B.
Target genes for Polycomb components
6440
750
Ring1B
237
H3K27me3
6740
450
Ezh2
32
H3K27me3
6885
305
Suz12
2
H3K27me3
C.
H3K27me3 at PRC2 targets
Reads per bin per million
-25kb TSS TES 25kb
D0 ESCs
D4 EBs
D8 EBs
H3K27me3 CJ7 Ezh2WT
H3K27me3 CJ7 Ezh2681C-99
IgG CJ7 Ezh2WT
D.
PRC2 TARGETS RNA-seq
Activated
Mtase independent
Mtase dependent
CJ7 Ezh2WT CJ7 Ezh2681C-99
D0 D4 D8 D0 D4 D8
367
218
-2 0 2
z-scores of RPKM
Repressed
183
167
E.
H3K27me3 atPRC2 developmentally repressed genes
CJ7 Ezh2WT
CJ7 Ezh2681C-99
Normalized tag density
Day 0
Day 4
Day 8
-3kb TSS +3kb
Mtase independent
Mtase dependent

587

Figure 4.

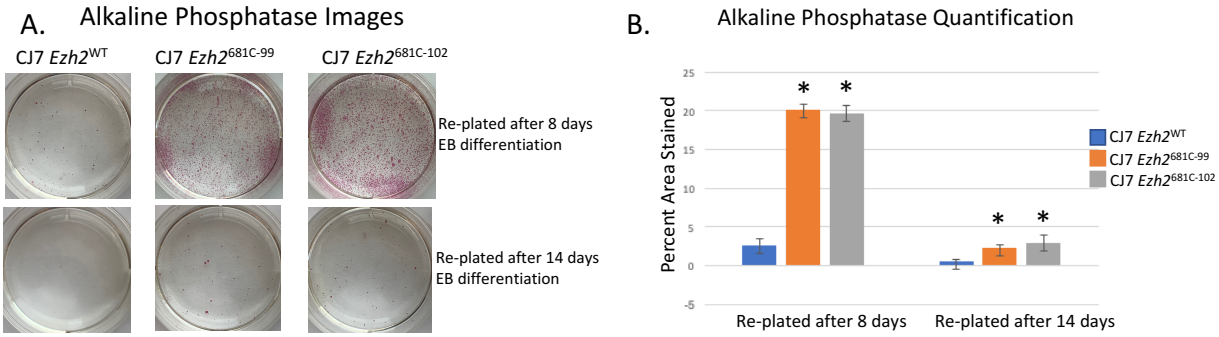

588

589

Figure 5.

A.

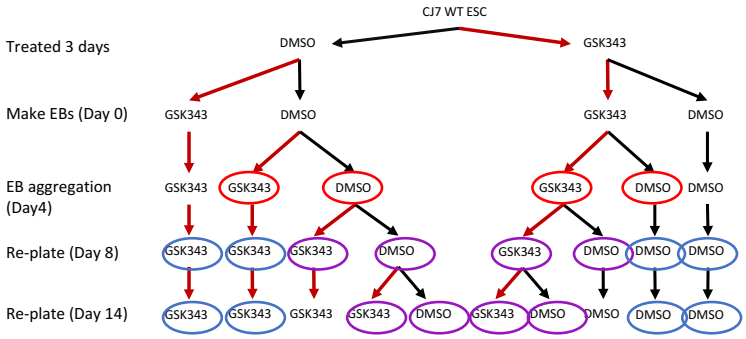

B.

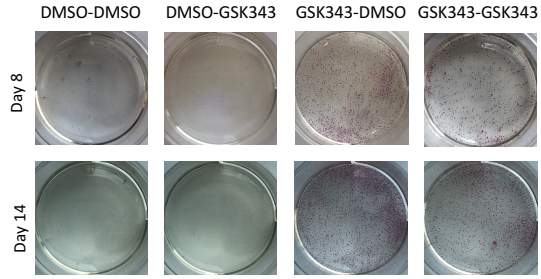

C.

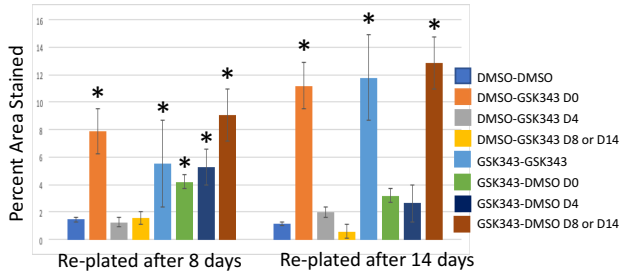

D.

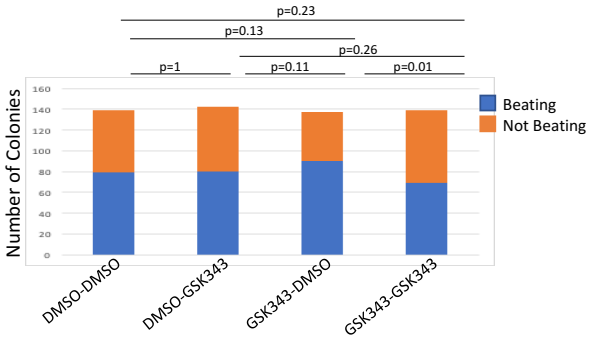

E.

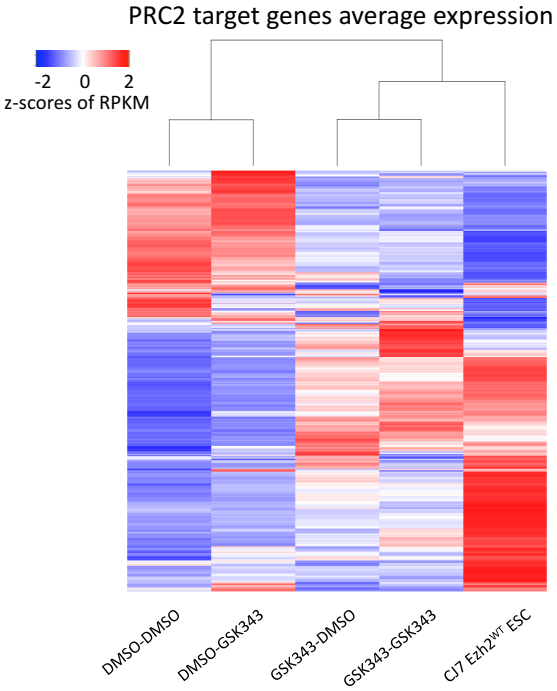

590

591

592 Figure Legends:

593

594 Figure 1

595 (A) Diagram of embryoid body (EB) formation time-course. (B) Western blot of cells treated
596 with GSK343 EZH2 inhibitor or DMSO control probed with H3K27me3 and EZH2 antibodies. (C)
597 54x magnification of day 4 EBs from cells treated with either DMSO control or GSK343. (D)
598 Screen shots from RNA-seq over the EB differentiation time-course from Mtase independent
599 (Sox3 and Tbx3) and Mtase dependent (Itgb7 and Wnt3) genes from cells treated with DMSO
600 (blue) or GSK343 (red). (E) Heatmap showing expression patterns of Mtase dependent and
601 independent genes in untreated (DMSO) and treated (GSK343) ES cells over development time-
602 course. Z-scores of average RPKMs of duplicates are shown for each gene across all samples.
603 Genes are separated based on if they were activated (top) or repressed (bottom) in untreated
604 cells over time as well as if they had a similar expression pattern in treated cells (Mtase
605 dependent genes) (left) or a different expression pattern (Mtase independent genes) (right).
606 The four groups are further clustered based on fold-changes over time in untreated cells.

607

608 Figure 2

609 (A) Diagram of *Ezh2* SET domain structure with the 681 residue circled and an alignment of SET
610 domains with the analogous residue highlighted in red adapted from (Antonysamy et al., 2013).
611 It is highly conserved across species and methyltransferases. (B) In vitro methyltransferase
612 assay with PRC2 comprised of WT or mutant EZH2, EED, SUZ12, and RBAP48. Recombinant H3 is
613 the substrate and a radioactive SAM was the methyl donor. Reactions progressed for 1 or 6
614 hours. (C) Western blot from WT, mutant and PRC2 knockout cells probed with H3K27me and
615 EZH2 antibodies. (D) 54x magnification of embryonic stem cells (ESCs) or embryoid bodies that
616 have differentiated for 4 days (Day 4 EBs) from WT, 681C-99, 681C-102 and *Eed*$^{-/-}$ cells. (E) Venn
617 diagram showing the overlap in SUZ12 CUT&RUN peaks from WT and 681C-99 mutant ESCs. (F)
618 Venn diagram showing the overlaps in SUZ12 CUT&RUN peaks from WT and 681C-99 mutant
619 cells differentiated as embryoid bodies for 4 to 8 days. (G) Quantification of beating heart assay
620 from WT, 681C-99 and 681C-102 cells that were differentiated as EBs for 4 days and then

621 individually plated in differentiation media. Blue shows the number of EBs that gave rise to
622 beating cells and Orange shows those that did not.
623
624
625
626 Figure 3
627 (A) Venn diagram showing overlap of H3K27me3 target genes assigned from CUT&RUN peaks
628 from WT cells and published ChIP-seq data peaks. (B) Venn diagrams showing overlap of target
629 genes of H3K27me3 and other PRC2 components by CUT&RUN in WT cells. (C) Metaplots over
630 PRC2 target genes showing H3K27me3 CUT&RUN versus IgG control signal at Day 0, 4 and 8 of
631 embryoid body formation in wild-type and mutant cells. (D) Heatmap showing expression
632 patterns of Mtase dependent and independent genes in wild-type and mutant ES cells over
633 developmental time-course. Z-scores of average RPKMs of triplicates are shown for each gene
634 across all samples. Genes are separated based on if they were activated (left two panels) or
635 repressed (right two panels) in wild-type cells over time as well as if they had a similar
636 expression pattern in mutant cells (Mtase dependent genes) or a different expression pattern
637 (Mtase independent genes). The four groups are further clustered based on fold-changes over
638 time in untreated cells. (E) Metaplots showing H3K27me3 binding in wild-type and mutant cells
639 by cut-and-run at Mtase dependent or independent and developmentally repressed PRC2
640 target genes over the time course.
641
642 Figure 4
643 (A) Alkaline phosphatase staining from WT, 681C-99 and 681C-102 cells that had been
644 differentiated for 8 or 14 days and then transferred into ESC conditions for five days before
645 staining. ESCs stain bright pink in this assay. (B) Quantification of alkaline phosphatase staining
646 from re-plated cells with standard deviation error bars. Samples with significant difference
647 ($p<0.05$) from WT cells marked with an asterisk.
648
649

650 Figure 5

651 (A) Diagram showing the drug treatment plan for differentiation and re-plating of cells. Red
652 circles indicate the cells used for the beating heart assay in panel D, Purple are shown in images
653 in (B) as well as quantified in (C) and blue circles highlight samples only quantified in (C). (B)
654 Alkaline phosphatase staining from treated cells re-plated after 8 or 14 days of EB
655 differentiation. Only cells that start in GSK343 treatment stain pink indicating that the cells have
656 reverted to an ES phenotype. (C) Quantification of alkaline phosphatase staining from cells
657 treated with DMSO or GSK343. Time of the treatment switch is indicated in the legend. Samples
658 with significant differences from those continuously treated with DMSO ($p<0.05$) are marked
659 with an asterisk. (D) Quantification of beating heart assay with GSK343 and DMSO treated cells.
660 Cells were differentiated as EBs for 4 days and then plated into differentiation media. Blue
661 indicates the number of EBs that formed beating cells and orange indicates the number that did
662 not. (E) Unsupervised clustering of RNA-seq average expression of cells re-plated for 5 days
663 after 14 days of EB formation. Cells that were treated with GSK343 have gene expression
664 profiles that cluster with average expression from WT ESCs.

665

666

Supp. Fig. 1

A. GSK343 Titration 3 day treatment

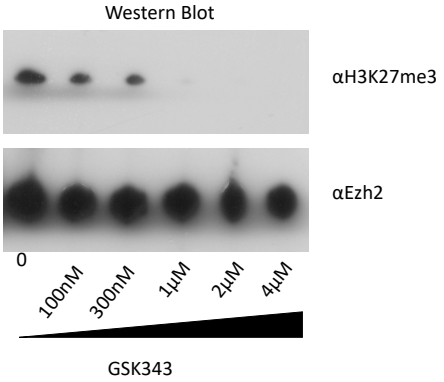

B. DMSO/GSK343 3 day treatment

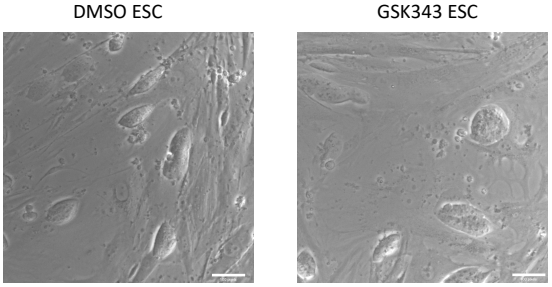

C.

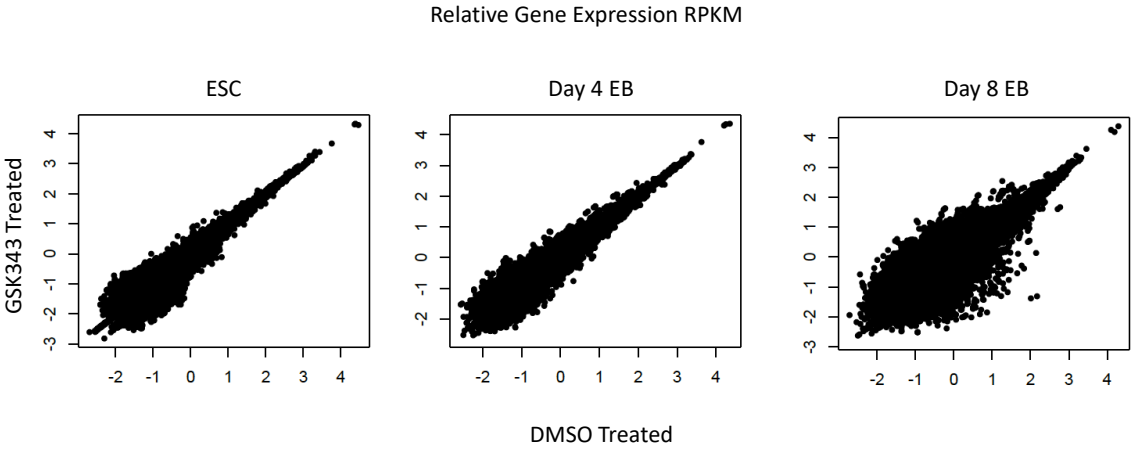

667

668

Supp. Fig. 2

A.

In vitro methyltransferase assay

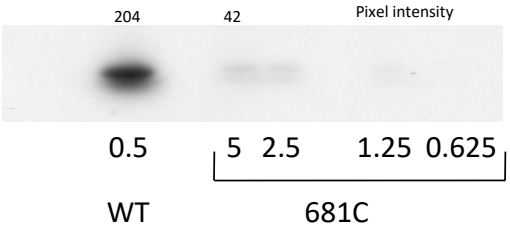

B. In vitro methyltransferase assay

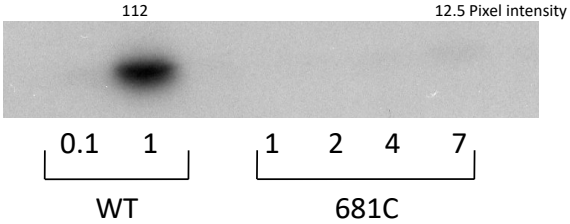

C.

In vitro Methyltransferase Assay

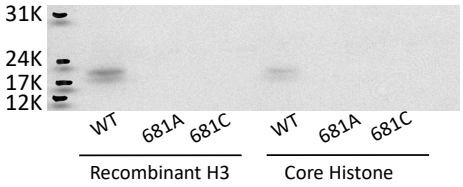

D. In vitro Methyltransferase Assay

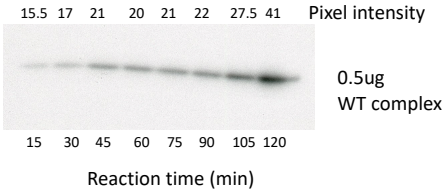

E. Protein purification

PRC2 Ezh2^{681C}

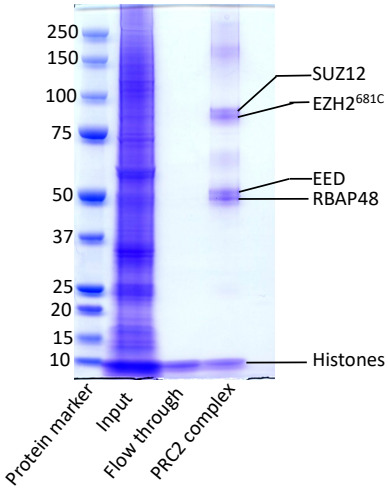

669

Supp. Fig. 3

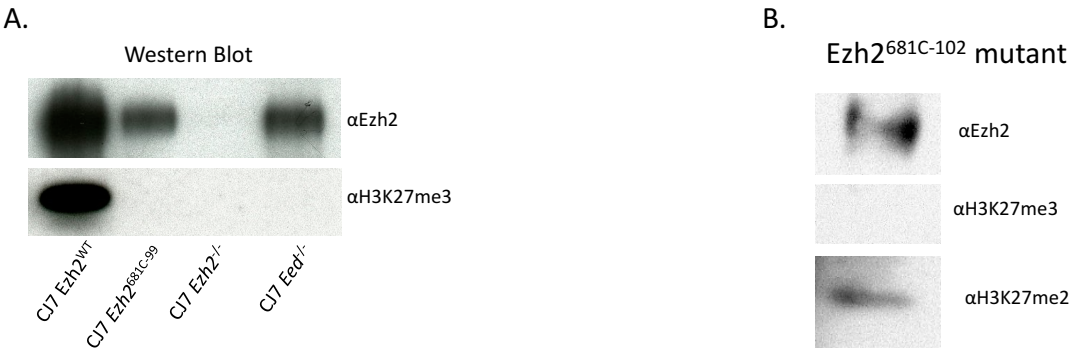

670

Supp. Fig. 4

A.

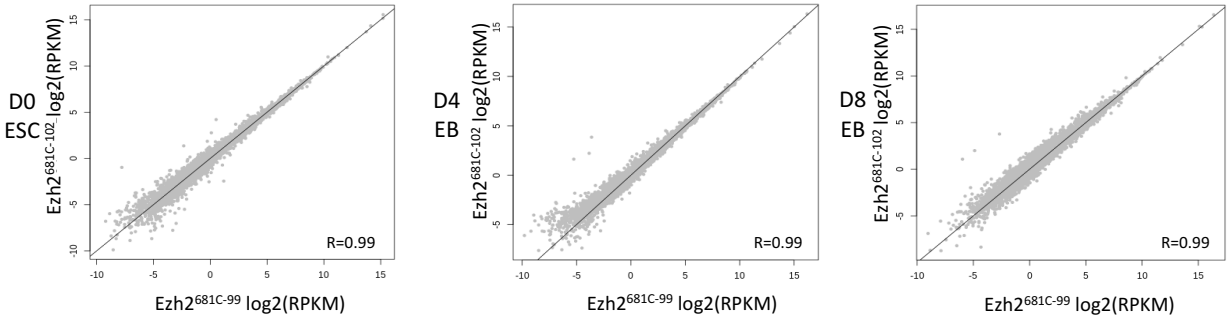

B.

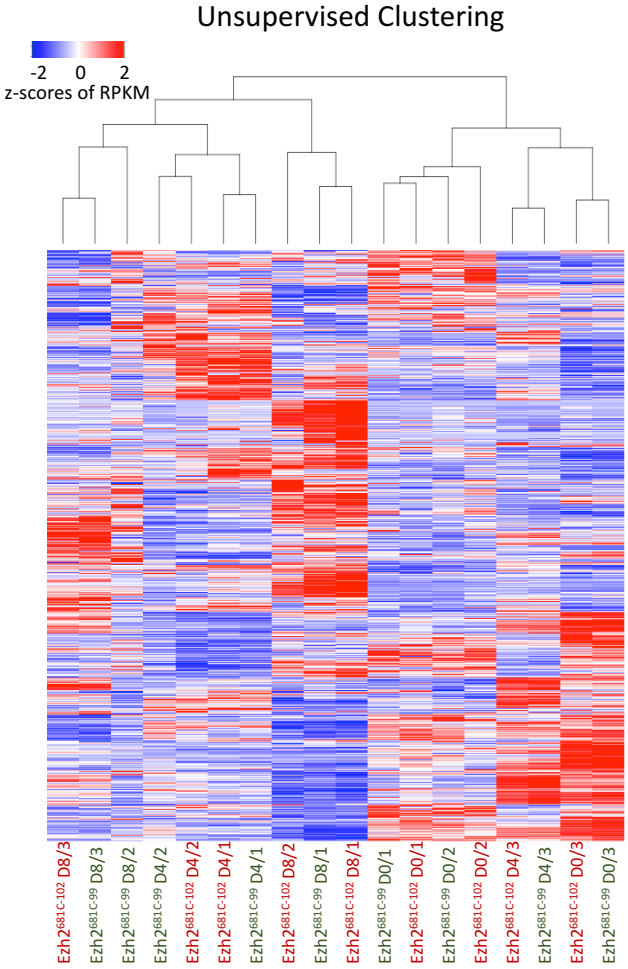

671

Supp. Fig. 5

Log2 fold-change as compared to WT comparisons between drug treated and mutant cells

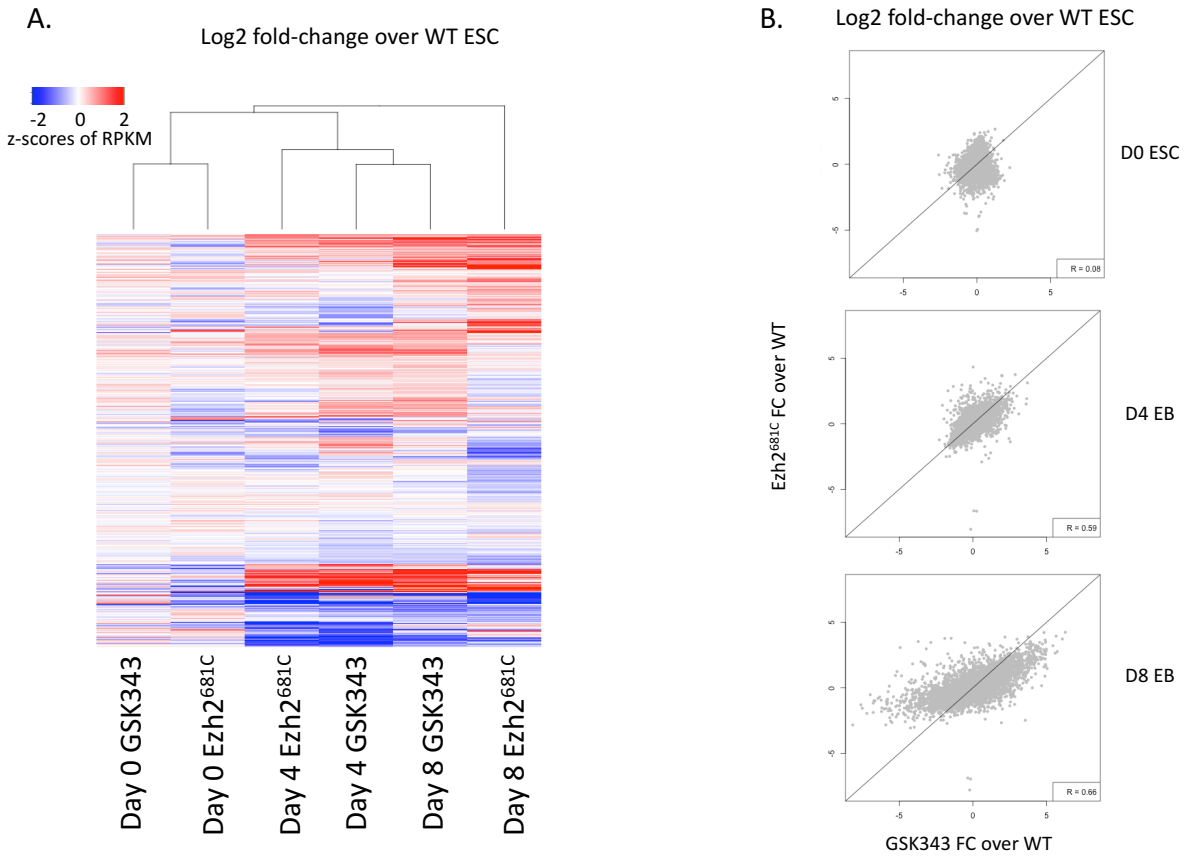

Supp. Fig. 6.

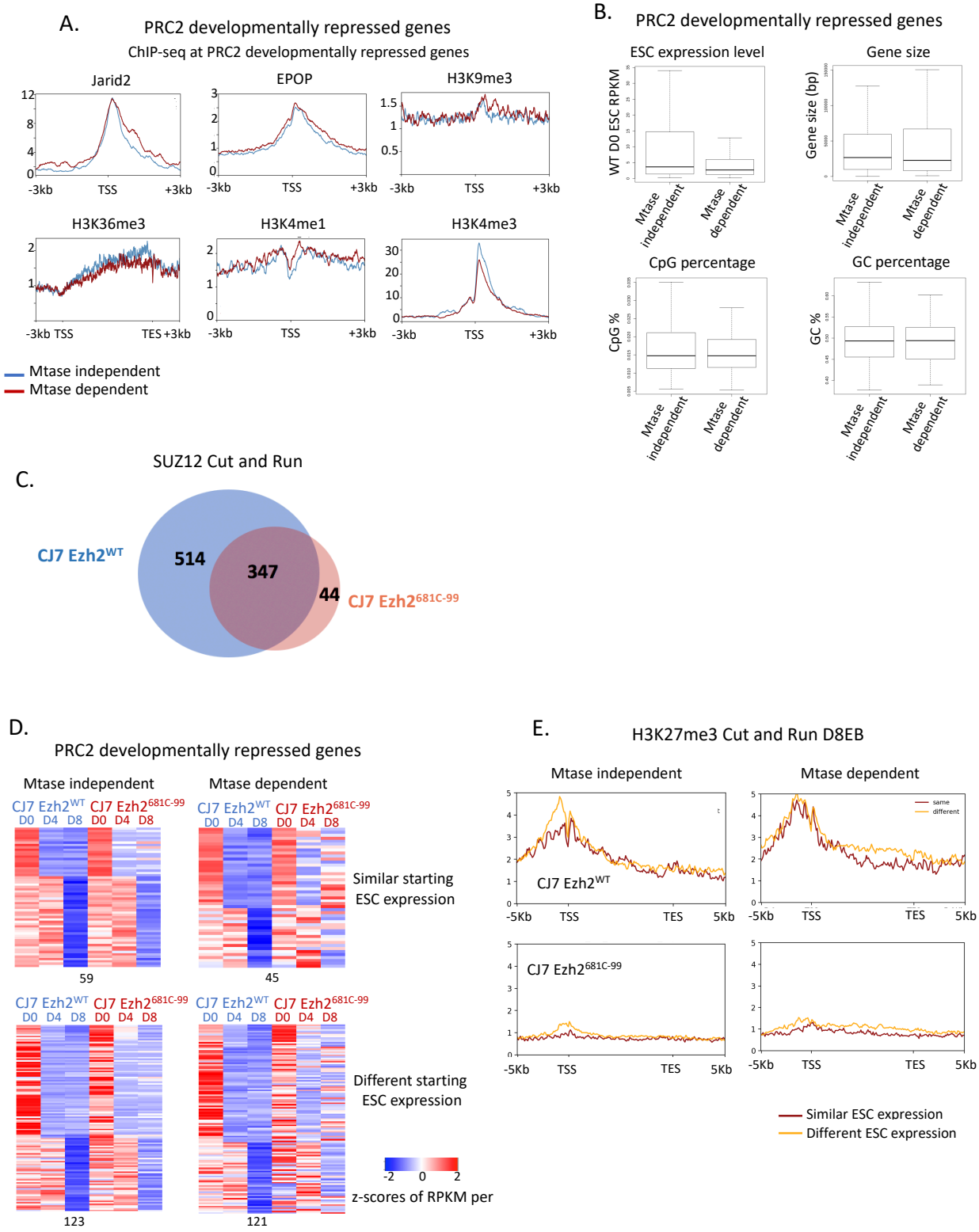

674

675

Supp. Fig. 7.

A.

Western Blot

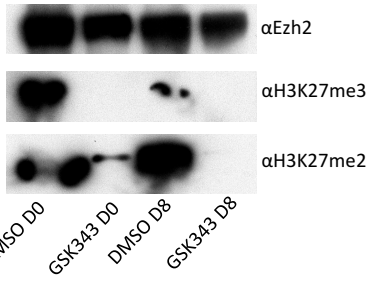

B.

14 Day re-plating RNA-seq samples

PRC2 target genes

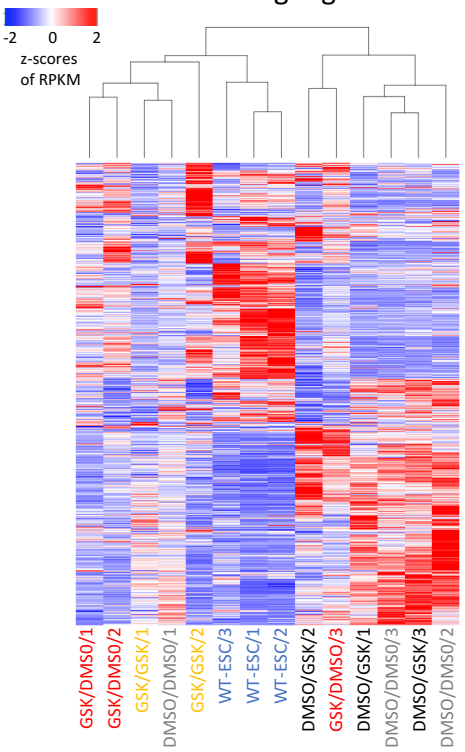

C.

14 Day re-plating RNA-seq samples

PRC2 developmentally repressed genes

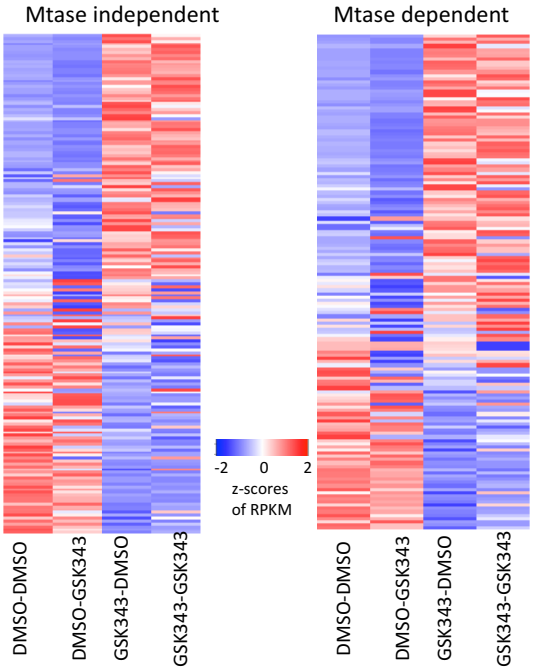

676

677

678 Supplemental Figure Legends

679

680 Supp. Fig. 1

681 (A) Western blot of WT CJ7 cells treated for three days with an increasing concentration of
682 GSK343 probed with antibodies to H3K27me3 and EZH2. The 4uM concentration was non-toxic
683 to cells and yielded a loss of H3K27me3 signal and so this concentration was used for all
684 experiments. (B) 54x magnification of ES cells treated for three days with DMSO or GSK343. ES
685 colonies show characteristic halo and are indistinguishable between treatments. (C)
686 Comparisons of normalized gene expression (RPKM) from cells treated with DMSO or GSK343
687 and differentiated as embryoid bodies. At the genome level there are many genes that have the
688 same expression pattern across the two treatments.

689

690 Supp. Fig. 2

691 (A,B) In vitro methyltransferase assay comparing EZH2-WT and EZH2-681C. Concentration of
692 the PRC2 complex is indicated below the image with pixel intensity indicated above. (C) In vitro
693 methyltransferase assay with WT, 681A and 681C complexes with both recombinant histones
694 that do not have any covalent modifications and core histones that do as the substrate. With
695 both substrates, the mutant complexes did not show signal. (D) In vitro methyltransferase assay
696 with WT complex over time. All other methyltransferase assays shown here were done for 60
697 minutes which is well within the linear range. (E) Coomassie stain of mutant PRC2 complex.
698 Complex was purified from Sf9 cells by using a Flag-tagged SUZ12 and purifying over flag beads.

699

700 Supp. Fig. 3

701 (A) Western blot showing the EZH2 and H3K27me3 signal for WT, EZH2 mutant and PRC2 KO
702 cells. (B) Western blot showing the EZH2, H3K27me3 and H3K27me2 signal of $EZH2^{618C-102}$
703 mutant cells.

704

705 Supp. Fig. 4

706 (A) Comparisons between Ezh2$^{618C-99}$ and Ezh2$^{681C-102}$ RNA-seq over the differentiation time-
707 course. The two mutants are nearly identical at all time points. (B) Unsupervised clustering of
708 the mutant RNA-seq showing that the day of differentiation is more relevant predictor of
709 similarity rather than the mutant strain.
710
711 Supp. Fig. 5
712 (A) Unsupervised clustering showing the fold change over WT ESC of GSK343 treated or
713 Ezh2681C-99 cells. The day of differentiation is the stronger predictor of clustering. (B) Direct
714 comparison of mutant and drug treated cells RNA-seq fold change over WT gene expression.
715
716 Supp. Fig. 6
717 (A) Average profiles showing binding of other PRC2 components and histone marks in wild-type
718 and mutant cells at Mtase dependent or independent and developmentally repressed PRC2
719 target genes over the time course. (B) Boxplots showing comparisons of different
720 characteristics of Mtase dependent and independent, developmentally repressed PRC2 target
721 genes in wild-type and mutant cells. (C) Venn diagram showing the overlap in SUZ12 peaks from
722 CUT&RUN experiments from WT and Ezh2$^{618C-99}$ cells. (D) Heatmaps showing developmentally
723 repressed genes from Fig 3D, separated based on expression levels of wild-type and mutant ES
724 cells at Day 0 of the time-course. Genes with similar expression levels at Day 0 in wild-type and
725 mutant (within 1.2 fold) are on the top and those with different starting expression levels (more
726 than 1.2 fold) are at the bottom. (E) Average profiles showing H3K27me3 binding in wild-type
727 and mutant cells by cut-and-run at Mtase dependent or independent and developmentally
728 repressed PRC2 target genes that have either different (more than 1.2 fold) or similar (within
729 1.2 fold) expression over the time course.
730
731 Supp. Fig. 7
732 (A) Western blot of CJ7 cells treated with DMSO or GSK343 showing the (levels of Ezh2,
733 H3K27me3 and H3K27me2 at Day 0 and Day 8 or EB formation. B) Unsupervised clustering of
734 PRC2 target genes in re-plated cells and wild-type ES-cells. Untreated or drug treated cells were

735 replated at 14 days in DMSO or GSK343. Z-scores of average RPKMs of triplicates (duplicates for
736 GSK-GSK) are shown for each gene across all samples. (C) Heatmaps showing comparison of
737 treated and untreated cells, re-plated in DMSO or GSK343 for previously identified Mtase
738 dependent and independent genes. Z-scores of average RPKMs of triplicates (duplicates for
739 GSK-GSK) are shown for each gene across all samples.
740
741
742
743 Abdel Raouf, S. M., Ibrahim, T. R., Abdelaziz, L. A., Farid, M. I., & Mohamed, S. Y. (2019, Dec 10).
744 Prognostic Value of TWIST1 and EZH2 Expression in Colon Cancer. *J Gastrointest Cancer*.
745 https://doi.org/10.1007/s12029-019-00344-4
746
747 Ahmed, A., Wang, T., & Delgado-Olguin, P. (2018). Ezh2 is not required for cardiac regeneration
748 in neonatal mice. *PLoS One, 13*(2), e0192238.
749 https://doi.org/10.1371/journal.pone.0192238
750
751 Ai, S., Peng, Y., Li, C., Gu, F., Yu, X., Yue, Y., Ma, Q., Chen, J., Lin, Z., Zhou, P., Xie, H., Prendiville,
752 T. W., Zheng, W., Liu, Y., Orkin, S. H., Wang, D. Z., Yu, J., Pu, W. T., & He, A. (2017, Apr
753 10). EED orchestration of heart maturation through interaction with HDACs is
754 H3K27me3-independent. *Elife, 6*. https://doi.org/10.7554/eLife.24570
755
756 Aloia, L., Di Stefano, B., & Di Croce, L. (2013, Jun). Polycomb complexes in stem cells and
757 embryonic development. *Development, 140*(12), 2525-2534.
758 https://doi.org/10.1242/dev.091553
759
760 Antonysamy, S., Condon, B., Druzina, Z., Bonanno, J. B., Gheyi, T., Zhang, F., MacEwan, I., Zhang,
761 A., Ashok, S., Rodgers, L., Russell, M., & Gately Luz, J. (2013). Structural context of
762 disease-associated mutations and putative mechanism of autoinhibition revealed by X-

763 ray crystallographic analysis of the EZH2-SET domain. *PLoS One, 8*(12), e84147.
764 https://doi.org/10.1371/journal.pone.0084147
765
766 Basheer, F., Giotopoulos, G., Meduri, E., Yun, H., Mazan, M., Sasca, D., Gallipoli, P., Marando, L.,
767 Gozdecka, M., Asby, R., Sheppard, O., Dudek, M., Bullinger, L., Dohner, H., Dillon, R.,
768 Freeman, S., Ottmann, O., Burnett, A., Russell, N., Papaemmanuil, E., Hills, R., Campbell,
769 P., Vassiliou, G. S., & Huntly, B. J. P. (2019, Apr 1). Contrasting requirements during
770 disease evolution identify EZH2 as a therapeutic target in AML. *J Exp Med, 216*(4), 966-
771 981. https://doi.org/10.1084/jem.20181276
772
773 Behringer, R., Gertsenstein, M., Nagy, K. V., & Nagy, A. (2016, Dec 1). Differentiating Mouse
774 Embryonic Stem Cells into Embryoid Bodies by Hanging-Drop Cultures. *Cold Spring Harb*
775 *Protoc, 2016*(12). https://doi.org/10.1101/pdb.prot092429
776
777 Beringer, M., Pisano, P., Di Carlo, V., Blanco, E., Chammas, P., Vizán, P., Gutiérrez, A., Aranda, S.,
778 Payer, B., Wierer, M., & Di Croce, L. (2016, Nov 17). EPOP Functionally Links Elongin and
779 Polycomb in Pluripotent Stem Cells. *Mol Cell, 64*(4), 645-658.
780 https://doi.org/10.1016/j.molcel.2016.10.018
781
782 Bernstein, E., Duncan, E. M., Masui, O., Gil, J., Heard, E., & Allis, C. D. (2006, Apr). Mouse
783 polycomb proteins bind differentially to methylated histone H3 and RNA and are
784 enriched in facultative heterochromatin. *Mol Cell Biol, 26*(7), 2560-2569.
785 https://doi.org/10.1128/mcb.26.7.2560-2569.2006
786
787 Boheler, K. R., Czyz, J., Tweedie, D., Yang, H. T., Anisimov, S. V., & Wobus, A. M. (2002, Aug 9).
788 Differentiation of pluripotent embryonic stem cells into cardiomyocytes. *Circ Res, 91*(3),
789 189-201. https://doi.org/10.1161/01.res.0000027865.61704.32
790

791 Bohm, J., Muenzner, J. K., Caliskan, A., Ndreshkjana, B., Erlenbach-Wunsch, K., Merkel, S.,
792 Croner, R., Rau, T. T., Geppert, C. I., Hartmann, A., Roehe, A. V., & Schneider-Stock, R.
793 (2019, Sep). Loss of enhancer of zeste homologue 2 (EZH2) at tumor invasion front is
794 correlated with higher aggressiveness in colorectal cancer cells. *J Cancer Res Clin Oncol,*
795 *145*(9), 2227-2240. https://doi.org/10.1007/s00432-019-02977-1
796
797 Bowman, S. K., Simon, M. D., Deaton, A. M., Tolstorukov, M., Borowsky, M. L., & Kingston, R. E.
798 (2013, Jul 9). Multiplexed Illumina sequencing libraries from picogram quantities of
799 DNA. *BMC Genomics, 14*, 466. https://doi.org/10.1186/1471-2164-14-466
800
801 Bradley, W. D., Arora, S., Busby, J., Balasubramanian, S., Gehling, V. S., Nasveschuk, C. G.,
802 Vaswani, R. G., Yuan, C. C., Hatton, C., Zhao, F., Williamson, K. E., Iyer, P., Méndez, J.,
803 Campbell, R., Cantone, N., Garapaty-Rao, S., Audia, J. E., Cook, A. S., Dakin, L. A.,
804 Albrecht, B. K., Harmange, J. C., Daniels, D. L., Cummings, R. T., Bryant, B. M., Normant,
805 E., & Trojer, P. (2014, Nov 20). EZH2 inhibitor efficacy in non-Hodgkin's lymphoma does
806 not require suppression of H3K27 monomethylation. *Chem Biol, 21*(11), 1463-1475.
807 https://doi.org/10.1016/j.chembiol.2014.09.017
808
809 Bremer, S. C. B., Conradi, L. C., Mechie, N. C., Amanzada, A., Mavropoulou, E., Kitz, J., Ghadimi,
810 M., Ellenrieder, V., Strobel, P., Hessmann, E., Gaedcke, J., & Bohnenberger, H. (2019,
811 Nov 6). Enhancer of Zeste Homolog 2 in Colorectal Cancer Development and
812 Progression. *Digestion*, 1-9. https://doi.org/10.1159/000504093
813
814 Chamberlain, S. J., Yee, D., & Magnuson, T. (2008, Jun). Polycomb repressive complex 2 is
815 dispensable for maintenance of embryonic stem cell pluripotency. *Stem Cells, 26*(6),
816 1496-1505. https://doi.org/10.1634/stemcells.2008-0102
817
818 Collinson, A., Collier, A. J., Morgan, N. P., Sienerth, A. R., Chandra, T., Andrews, S., & Rugg-Gunn,
819 P. J. (2016, Dec 6). Deletion of the Polycomb-Group Protein EZH2 Leads to Compromised

820 Self-Renewal and Differentiation Defects in Human Embryonic Stem Cells. *Cell Rep,*
821 *17*(10), 2700-2714. https://doi.org/10.1016/j.celrep.2016.11.032
822
823 Cyrus, S., Burkardt, D., Weaver, D. D., & Gibson, W. T. (2019, Dec). PRC2-complex related
824 dysfunction in overgrowth syndromes: A review of EZH2, EED, and SUZ12 and their
825 syndromic phenotypes. *Am J Med Genet C Semin Med Genet, 181*(4), 519-531.
826 https://doi.org/10.1002/ajmg.c.31754
827
828 Dang, S. M., Kyba, M., Perlingeiro, R., Daley, G. Q., & Zandstra, P. W. (2002, May 20). Efficiency
829 of embryoid body formation and hematopoietic development from embryonic stem
830 cells in different culture systems. *Biotechnol Bioeng, 78*(4), 442-453.
831 https://doi.org/10.1002/bit.10220
832
833 Deng, Y., Chen, X., Huang, C., Chen, G., Chen, F., Lu, J., Shi, X., He, C., Zeng, Z., Qiu, Y., Chen, J.,
834 Lin, R., Chen, Y., & Chen, J. (2019). EZH2/Bcl-2 Coexpression Predicts Worse Survival in
835 Diffuse Large B-cell Lymphomas and Demonstrates Poor Efficacy to Rituximab in
836 Localized Lesions. *J Cancer, 10*(9), 2006-2017. https://doi.org/10.7150/jca.29807
837
838 Dessau, R. B., & Pipper, C. B. (2008, Jan 28). ["R"--project for statistical computing]. *Ugeskr*
839 *Laeger, 170*(5), 328-330. (R--en programpakke til statistisk databehandling og grafik.)
840
841 Dobin, A., Davis, C. A., Schlesinger, F., Drenkow, J., Zaleski, C., Jha, S., Batut, P., Chaisson, M., &
842 Gingeras, T. R. (2013, Jan 1). STAR: ultrafast universal RNA-seq aligner. *Bioinformatics,*
843 *29*(1), 15-21. https://doi.org/10.1093/bioinformatics/bts635
844
845 Dou, D., Ge, X., Wang, X., Xu, X., Zhang, Z., Seng, J., Cao, Z., Gu, Y., & Han, M. (2019). EZH2
846 Contributes To Cisplatin Resistance In Breast Cancer By Epigenetically Suppressing miR-
847 381 Expression. *Onco Targets Ther, 12*, 9627-9637. https://doi.org/10.2147/ott.S214104
848

849 Ferguson, J., Devarajan, M., DiNuoscio, G., Saiakhova, A., Liu, C. F., Lefebvre, V., Scacheri, P. C.,
850 & Atit, R. P. (2018, Feb 2). PRC2 Is Dispensable in Vivo for β-Catenin-Mediated
851 Repression of Chondrogenesis in the Mouse Embryonic Cranial Mesenchyme. *G3*
852 *(Bethesda), 8*(2), 491-503. https://doi.org/10.1534/g3.117.300311
853
854 Fioravanti, R., Stazi, G., Zwergel, C., Valente, S., & Mai, A. (2018, Dec). Six Years (2012-2018) of
855 Researches on Catalytic EZH2 Inhibitors: The Boom of the 2-Pyridone Compounds. *Chem*
856 *Rec, 18*(12), 1818-1832. https://doi.org/10.1002/tcr.201800091
857
858 Fraineau, S., Palii, C. G., McNeill, B., Ritso, M., Shelley, W. C., Prasain, N., Chu, A., Vion, E., Rieck,
859 K., Nilufar, S., Perkins, T. J., Rudnicki, M. A., Allan, D. S., Yoder, M. C., Suuronen, E. J., &
860 Brand, M. (2017, Nov 14). Epigenetic Activation of Pro-angiogenic Signaling Pathways in
861 Human Endothelial Progenitors Increases Vasculogenesis. *Stem Cell Reports, 9*(5), 1573-
862 1587. https://doi.org/10.1016/j.stemcr.2017.09.009
863
864 Harris, J. (2018). Partial Clinical Hold on Tazemetostat Trials Lifted by FDA [News article].
865 *Targeted Oncology*.
866
867 Healy, E., Mucha, M., Glancy, E., Fitzpatrick, D. J., Conway, E., Neikes, H. K., Monger, C., Van
868 Mierlo, G., Baltissen, M. P., Koseki, Y., Vermeulen, M., Koseki, H., & Bracken, A. P. (2019,
869 Nov 7). PRC2.1 and PRC2.2 Synergize to Coordinate H3K27 Trimethylation. *Mol Cell,*
870 *76*(3), 437-452.e436. https://doi.org/10.1016/j.molcel.2019.08.012
871
872 Heinz, S., Benner, C., Spann, N., Bertolino, E., Lin, Y. C., Laslo, P., Cheng, J. X., Murre, C., Singh,
873 H., & Glass, C. K. (2010, May 28). Simple combinations of lineage-determining
874 transcription factors prime cis-regulatory elements required for macrophage and B cell
875 identities. *Mol Cell, 38*(4), 576-589. https://doi.org/10.1016/j.molcel.2010.05.004
876

877 Hescheler, J., Fleischmann, B. K., Lentini, S., Maltsev, V. A., Rohwedel, J., Wobus, A. M., &
878 Addicks, K. (1997, Nov). Embryonic stem cells: a model to study structural and functional
879 properties in cardiomyogenesis. *Cardiovasc Res, 36*(2), 149-162.
880 https://doi.org/10.1016/s0008-6363(97)00193-4
881
882 Hon, G. C., Song, C. X., Du, T., Jin, F., Selvaraj, S., Lee, A. Y., Yen, C. A., Ye, Z., Mao, S. Q., Wang,
883 B. A., Kuan, S., Edsall, L. E., Zhao, B. S., Xu, G. L., He, C., & Ren, B. (2014, Oct 23). 5mC
884 oxidation by Tet2 modulates enhancer activity and timing of transcriptome
885 reprogramming during differentiation. *Mol Cell, 56*(2), 286-297.
886 https://doi.org/10.1016/j.molcel.2014.08.026
887
888 Hunt, S. E., McLaren, W., Gil, L., Thormann, A., Schuilenburg, H., Sheppard, D., Parton, A.,
889 Armean, I. M., Trevanion, S. J., Flicek, P., & Cunningham, F. (2018, Jan 1). Ensembl
890 variation resources. *Database (Oxford), 2018*. https://doi.org/10.1093/database/bay119
891
892 Italiano, A., Soria, J. C., Toulmonde, M., Michot, J. M., Lucchesi, C., Varga, A., Coindre, J. M.,
893 Blakemore, S. J., Clawson, A., Suttle, B., McDonald, A. A., Woodruff, M., Ribich, S.,
894 Hedrick, E., Keilhack, H., Thomson, B., Owa, T., Copeland, R. A., Ho, P. T. C., & Ribrag, V.
895 (2018, May). Tazemetostat, an EZH2 inhibitor, in relapsed or refractory B-cell non-
896 Hodgkin lymphoma and advanced solid tumours: a first-in-human, open-label, phase 1
897 study. *Lancet Oncol, 19*(5), 649-659. https://doi.org/10.1016/s1470-2045(18)30145-1
898
899 Jain, P., & Di Croce, L. (2016, May). Mutations and deletions of PRC2 in prostate cancer.
900 *Bioessays, 38*(5), 446-454. https://doi.org/10.1002/bies.201500162
901
902 Juan, A. H., Wang, S., Ko, K. D., Zare, H., Tsai, P. F., Feng, X., Vivanco, K. O., Ascoli, A. M.,
903 Gutierrez-Cruz, G., Krebs, J., Sidoli, S., Knight, A. L., Pedersen, R. A., Garcia, B. A.,
904 Casellas, R., Zou, J., & Sartorelli, V. (2016, Oct 25). Roles of H3K27me2 and H3K27me3

905 Examined during Fate Specification of Embryonic Stem Cells. *Cell Rep, 17*(5), 1369-1382.
906 https://doi.org/10.1016/j.celrep.2016.09.087
907
908 Karlowee, V., Amatya, V. J., Takayasu, T., Takano, M., Yonezawa, U., Takeshima, Y., Sugiyama,
909 K., Kurisu, K., & Yamasaki, F. (2019). Immunostaining of Increased Expression of
910 Enhancer of Zeste Homolog 2 (EZH2) in Diffuse Midline Glioma H3K27M-Mutant
911 Patients with Poor Survival. *Pathobiology, 86*(2-3), 152-161.
912 https://doi.org/10.1159/000496691
913
914 Kondo, Y. (2014, Nov). Targeting histone methyltransferase EZH2 as cancer treatment. *J*
915 *Biochem, 156*(5), 249-257. https://doi.org/10.1093/jb/mvu054
916
917 Krill, L., Deng, W., Eskander, R., Mutch, D., Zweizig, S., Hoang, B., Ioffe, O., Randall, L., Lankes,
918 H., Miller, D. S., & Birrer, M. (2020, Feb). Overexpression of enhance of Zeste homolog 2
919 (EZH2) in endometrial carcinoma: An NRG Oncology/Gynecologic Oncology Group Study.
920 *Gynecol Oncol, 156*(2), 423-429. https://doi.org/10.1016/j.ygyno.2019.12.003
921
922 Lavarone, E., Barbieri, C. M., & Pasini, D. (2019, Apr 11). Dissecting the role of H3K27
923 acetylation and methylation in PRC2 mediated control of cellular identity. *Nat Commun,*
924 *10*(1), 1679. https://doi.org/10.1038/s41467-019-09624-w
925
926 Lewis, E., & Mislove, R. (1947). New mutants report. *Drosophila Information Service, 21*, 69.
927
928 Li, G., Margueron, R., Ku, M., Chambon, P., Bernstein, B. E., & Reinberg, D. (2010, Feb 15). Jarid2
929 and PRC2, partners in regulating gene expression. *Genes Dev, 24*(4), 368-380.
930 https://doi.org/10.1101/gad.1886410
931

932 Li, H., Handsaker, B., Wysoker, A., Fennell, T., Ruan, J., Homer, N., Marth, G., Abecasis, G., &
933 Durbin, R. (2009, Aug 15). The Sequence Alignment/Map format and SAMtools.
934 *Bioinformatics, 25*(16), 2078-2079. https://doi.org/10.1093/bioinformatics/btp352
935
936 Liao, Y., Smyth, G. K., & Shi, W. (2014, Apr 1). featureCounts: an efficient general purpose
937 program for assigning sequence reads to genomic features. *Bioinformatics, 30*(7), 923-
938 930. https://doi.org/10.1093/bioinformatics/btt656
939
940 Liu, T. P., Lo, H. L., Wei, L. S., Hsiao, H. H., & Yang, P. M. (2015, Feb). S-Adenosyl-L-methionine-
941 competitive inhibitors of the histone methyltransferase EZH2 induce autophagy and
942 enhance drug sensitivity in cancer cells. *Anticancer Drugs, 26*(2), 139-147.
943 https://doi.org/10.1097/cad.0000000000000166
944
945 Lue, J. K., & Amengual, J. E. (2018, Oct). Emerging EZH2 Inhibitors and Their Application in
946 Lymphoma. *Curr Hematol Malig Rep, 13*(5), 369-382. https://doi.org/10.1007/s11899-
947 018-0466-6
948
949 Margueron, R., Li, G., Sarma, K., Blais, A., Zavadil, J., Woodcock, C. L., Dynlacht, B. D., &
950 Reinberg, D. (2008, Nov 21). Ezh1 and Ezh2 maintain repressive chromatin through
951 different mechanisms. *Mol Cell, 32*(4), 503-518.
952 https://doi.org/10.1016/j.molcel.2008.11.004
953
954 Margueron, R., & Reinberg, D. (2011, Jan 20). The Polycomb complex PRC2 and its mark in life.
955 *Nature, 469*(7330), 343-349. https://doi.org/10.1038/nature09784
956
957 Matsubara, T., Toyokawa, G., Takada, K., Kinoshita, F., Kozuma, Y., Akamine, T., Shimokawa, M.,
958 Haro, A., Osoegawa, A., Tagawa, T., & Mori, M. (2019). The association and prognostic
959 impact of enhancer of zeste homologue 2 expression and epithelial-mesenchymal

960 transition in resected lung adenocarcinoma. *PLoS One, 14*(5), e0215103.
961 https://doi.org/10.1371/journal.pone.0215103
962
963 Mechaal, A., Menif, S., Abbes, S., & Safra, I. (2019, Sep). EZH2, new diagnosis and prognosis
964 marker in acute myeloid leukemia patients. *Adv Med Sci, 64*(2), 395-401.
965 https://doi.org/10.1016/j.advms.2019.07.002
966
967 Nakagawa, M., Koyanagi, M., Tanabe, K., Takahashi, K., Ichisaka, T., Aoi, T., Okita, K., Mochiduki,
968 Y., Takizawa, N., & Yamanaka, S. (2008, Jan). Generation of induced pluripotent stem
969 cells without Myc from mouse and human fibroblasts. *Nat Biotechnol, 26*(1), 101-106.
970 https://doi.org/10.1038/nbt1374
971
972 O'Geen, H., Ren, C., Nicolet, C. M., Perez, A. A., Halmai, J., Le, V. M., Mackay, J. P., Farnham, P.
973 J., & Segal, D. J. (2017, Sep 29). dCas9-based epigenome editing suggests acquisition of
974 histone methylation is not sufficient for target gene repression. *Nucleic Acids Res,*
975 *45*(17), 9901-9916. https://doi.org/10.1093/nar/gkx578
976
977 Oksuz, O., Narendra, V., Lee, C. H., Descostes, N., LeRoy, G., Raviram, R., Blumenberg, L., Karch,
978 K., Rocha, P. P., Garcia, B. A., Skok, J. A., & Reinberg, D. (2018, Jun 21). Capturing the
979 Onset of PRC2-Mediated Repressive Domain Formation. *Mol Cell, 70*(6), 1149-
980 1162.e1145. https://doi.org/10.1016/j.molcel.2018.05.023
981
982 Pasini, D., Bracken, A. P., Hansen, J. B., Capillo, M., & Helin, K. (2007, May). The polycomb group
983 protein Suz12 is required for embryonic stem cell differentiation. *Mol Cell Biol, 27*(10),
984 3769-3779. https://doi.org/10.1128/mcb.01432-06
985
986 Pasini, D., Bracken, A. P., Jensen, M. R., Lazzerini Denchi, E., & Helin, K. (2004, Oct 13). Suz12 is
987 essential for mouse development and for EZH2 histone methyltransferase activity. *Embo*
988 *j, 23*(20), 4061-4071. https://doi.org/10.1038/sj.emboj.7600402

989

990 Pereira, C. F., Piccolo, F. M., Tsubouchi, T., Sauer, S., Ryan, N. K., Bruno, L., Landeira, D., Santos,
991 J., Banito, A., Gil, J., Koseki, H., Merkenschlager, M., & Fisher, A. G. (2010, Jun 4). ESCs
992 require PRC2 to direct the successful reprogramming of differentiated cells toward
993 pluripotency. *Cell Stem Cell, 6*(6), 547-556. https://doi.org/10.1016/j.stem.2010.04.013
994

995 Qi, W., Chan, H., Teng, L., Li, L., Chuai, S., Zhang, R., Zeng, J., Li, M., Fan, H., Lin, Y., Gu, J.,
996 Ardayfio, O., Zhang, J. H., Yan, X., Fang, J., Mi, Y., Zhang, M., Zhou, T., Feng, G., Chen, Z.,
997 Li, G., Yang, T., Zhao, K., Liu, X., Yu, Z., Lu, C. X., Atadja, P., & Li, E. (2012, Dec 26).
998 Selective inhibition of Ezh2 by a small molecule inhibitor blocks tumor cells proliferation.
999 *Proc Natl Acad Sci U S A, 109*(52), 21360-21365.
1000 https://doi.org/10.1073/pnas.1210371110
1001

1002 Rai, A. N., Vargas, M. L., Wang, L., Andersen, E. F., Miller, E. L., & Simon, J. A. (2013, Dec).
1003 Elements of the polycomb repressor SU(Z)12 needed for histone H3-K27 methylation,
1004 the interface with E(Z), and in vivo function. *Mol Cell Biol, 33*(24), 4844-4856.
1005 https://doi.org/10.1128/mcb.00307-13
1006

1007 Ramírez, F., Dündar, F., Diehl, S., Grüning, B. A., & Manke, T. (2014, Jul). deepTools: a flexible
1008 platform for exploring deep-sequencing data. *Nucleic Acids Res, 42*(Web Server issue),
1009 W187-191. https://doi.org/10.1093/nar/gku365
1010

1011 Robinson, J. T., Thorvaldsdóttir, H., Winckler, W., Guttman, M., Lander, E. S., Getz, G., &
1012 Mesirov, J. P. (2011, Jan). Integrative genomics viewer. *Nat Biotechnol, 29*(1), 24-26.
1013 https://doi.org/10.1038/nbt.1754
1014

1015 Robinson, M. D., McCarthy, D. J., & Smyth, G. K. (2010, Jan 1). edgeR: a Bioconductor package
1016 for differential expression analysis of digital gene expression data. *Bioinformatics, 26*(1),
1017 139-140. https://doi.org/10.1093/bioinformatics/btp616

1018

1019 Schuettengruber, B., Bourbon, H. M., Di Croce, L., & Cavalli, G. (2017, Sep 21). Genome
1020 Regulation by Polycomb and Trithorax: 70 Years and Counting. *Cell, 171*(1), 34-57.
1021 https://doi.org/10.1016/j.cell.2017.08.002

1022

1023 Shan, Y., Liang, Z., Xing, Q., Zhang, T., Wang, B., Tian, S., Huang, W., Zhang, Y., Yao, J., Zhu, Y.,
1024 Huang, K., Liu, Y., Wang, X., Chen, Q., Zhang, J., Shang, B., Li, S., Shi, X., Liao, B., Zhang,
1025 C., Lai, K., Zhong, X., Shu, X., Wang, J., Yao, H., Chen, J., Pei, D., & Pan, G. (2017, Sep 22).
1026 PRC2 specifies ectoderm lineages and maintains pluripotency in primed but not naïve
1027 ESCs. *Nat Commun, 8*(1), 672. https://doi.org/10.1038/s41467-017-00668-4

1028

1029 Shen, X., Kim, W., Fujiwara, Y., Simon, M. D., Liu, Y., Mysliwiec, M. R., Yuan, G. C., Lee, Y., &
1030 Orkin, S. H. (2009, Dec 24). Jumonji modulates polycomb activity and self-renewal
1031 versus differentiation of stem cells. *Cell, 139*(7), 1303-1314.
1032 https://doi.org/10.1016/j.cell.2009.12.003

1033

1034 Shen, X., Liu, Y., Hsu, Y. J., Fujiwara, Y., Kim, J., Mao, X., Yuan, G. C., & Orkin, S. H. (2008, Nov
1035 21). EZH1 mediates methylation on histone H3 lysine 27 and complements EZH2 in
1036 maintaining stem cell identity and executing pluripotency. *Mol Cell, 32*(4), 491-502.
1037 https://doi.org/10.1016/j.molcel.2008.10.016

1038

1039 Shi, B., Behrens, C., Vaghani, V., Riquelme, E. M., Rodriguez-Canales, J., Kadara, H., Lin, H., Lee,
1040 J., Liu, H., Wistuba, I., & Simon, G. (2019, Oct). Oncogenic enhancer of zeste homolog 2
1041 is an actionable target in patients with non-small cell lung cancer. *Cancer Med, 8*(14),
1042 6383-6392. https://doi.org/10.1002/cam4.1855

1043

1044 Skene, P. J., & Henikoff, S. (2017, Jan 16). An efficient targeted nuclease strategy for high-
1045 resolution mapping of DNA binding sites. *Elife, 6*. https://doi.org/10.7554/eLife.21856

1046

1047 Takahashi, K., & Yamanaka, S. (2006, Aug 25). Induction of pluripotent stem cells from mouse
1048 embryonic and adult fibroblast cultures by defined factors. *Cell, 126*(4), 663-676.
1049 https://doi.org/10.1016/j.cell.2006.07.024
1050
1051 Thornton, S. R., Butty, V. L., Levine, S. S., & Boyer, L. A. (2014). Polycomb Repressive Complex 2
1052 regulates lineage fidelity during embryonic stem cell differentiation. *PLoS One, 9*(10),
1053 e110498. https://doi.org/10.1371/journal.pone.0110498
1054
1055 Tian, Z., Li, Z., Zhu, Y., Meng, L., Liu, F., Sang, M., & Wang, G. (2019, Aug). Hypermethylation-
1056 mediated inactivation of miR-124 predicts poor prognosis and promotes tumor growth
1057 at least partially through targeting EZH2/H3K27me3 in ESCC. *Clin Exp Metastasis, 36*(4),
1058 381-391. https://doi.org/10.1007/s10585-019-09974-1
1059
1060 van Mierlo, G., Veenstra, G. J. C., Vermeulen, M., & Marks, H. (2019, Aug). The Complexity of
1061 PRC2 Subcomplexes. *Trends Cell Biol, 29*(8), 660-671.
1062 https://doi.org/10.1016/j.tcb.2019.05.004
1063
1064 Wasenang, W., Puapairoj, A., Settasatian, C., Proungvitaya, S., & Limpaiboon, T. (2019, Jul).
1065 Overexpression of polycomb repressive complex 2 key components EZH2/SUZ12/EED as
1066 an unfavorable prognostic marker in cholangiocarcinoma. *Pathol Res Pract, 215*(7),
1067 152451. https://doi.org/10.1016/j.prp.2019.152451
1068
1069 Wassef, M., Luscan, A., Aflaki, S., Zielinski, D., Jansen, P., Baymaz, H. I., Battistella, A., Kersouani,
1070 C., Servant, N., Wallace, M. R., Romero, P., Kosmider, O., Just, P. A., Hivelin, M., Jacques,
1071 S., Vincent-Salomon, A., Vermeulen, M., Vidaud, M., Pasmant, E., & Margueron, R.
1072 (2019, Mar 26). EZH1/2 function mostly within canonical PRC2 and exhibit proliferation-
1073 dependent redundancy that shapes mutational signatures in cancer. *Proc Natl Acad Sci*
1074 *U S A, 116*(13), 6075-6080. https://doi.org/10.1073/pnas.1814634116
1075

1076 Wu, X., Scott, H., Carlsson, S. V., Sjoberg, D. D., Cerundolo, L., Lilja, H., Prevo, R., Rieunier, G.,
1077 Macaulay, V., Higgins, G. S., Verrill, C. L., Lamb, A. D., Cunliffe, V. T., Bountra, C., Hamdy,
1078 F. C., & Bryant, R. J. (2019, Jul). Increased EZH2 expression in prostate cancer is
1079 associated with metastatic recurrence following external beam radiotherapy. *Prostate,*
1080 *79*(10), 1079-1089. https://doi.org/10.1002/pros.23817
1081
1082 Xu, B., On, D. M., Ma, A., Parton, T., Konze, K. D., Pattenden, S. G., Allison, D. F., Cai, L.,
1083 Rockowitz, S., Liu, S., Liu, Y., Li, F., Vedadi, M., Frye, S. V., Garcia, B. A., Zheng, D., Jin, J.,
1084 & Wang, G. G. (2015, Jan 8). Selective inhibition of EZH2 and EZH1 enzymatic activity by
1085 a small molecule suppresses MLL-rearranged leukemia. *Blood, 125*(2), 346-357.
1086 https://doi.org/10.1182/blood-2014-06-581082
1087
1088 Xu, H., Zhang, L., Qian, X., Zhou, X., Yan, Y., Zhou, J., Ge, W., Albahde, M., & Wang, W. (2019,
1089 Oct). GSK343 induces autophagy and downregulates the AKT/mTOR signaling pathway
1090 in pancreatic cancer cells. *Exp Ther Med, 18*(4), 2608-2616.
1091 https://doi.org/10.3892/etm.2019.7845
1092
1093 Yamagishi, M., & Uchimaru, K. (2017, Sep). Targeting EZH2 in cancer therapy. *Curr Opin Oncol,*
1094 *29*(5), 375-381. https://doi.org/10.1097/cco.0000000000000390
1095
1096 Yang, P. M., Hong, Y. H., Hsu, K. C., & Liu, T. P. (2019). p38α/S1P/SREBP2 activation by the SAM-
1097 competitive EZH2 inhibitor GSK343 limits its anticancer activity but creates a druggable
1098 vulnerability in hepatocellular carcinoma. *Am J Cancer Res, 9*(10), 2120-2139.
1099
1100 Yu, W., Zhang, F., Wang, S., Fu, Y., Chen, J., Liang, X., Le, H., Pu, W. T., & Zhang, B. (2017, Apr
1101 13). Depletion of polycomb repressive complex 2 core component EED impairs fetal
1102 hematopoiesis. *Cell Death Dis, 8*(4), e2744. https://doi.org/10.1038/cddis.2017.163
1103

1104 Zhang, M. J., Chen, D. S., Li, H., Liu, W. W., Han, G. Y., & Han, Y. F. (2019). Clinical significance of
1105 USP7 and EZH2 in predicting prognosis of laryngeal squamous cell carcinoma and their
1106 possible functional mechanism. *Int J Clin Exp Pathol, 12*(6), 2184-2194.
1107
1108 Zhang, Q., Han, Q., Zi, J., Ma, J., Song, H., Tian, Y., McGrath, M., Song, C., & Ge, Z. (2019, Sep).
1109 Mutations in EZH2 are associated with poor prognosis for patients with myeloid
1110 neoplasms. *Genes Dis, 6*(3), 276-281. https://doi.org/10.1016/j.gendis.2019.05.001
1111
1112